IPN Progress Report 42-178 • August 15, 2009

The Planetary and Lunar Ephemeris DE 421

William M. Folkner,* James G. Williams,† and Dale H. Boggs†

The planetary and lunar ephemeris DE 421 represents updated estimates of the orbits of the Moon and planets. The lunar orbit is known to submeter accuracy through fitting lunar laser ranging data. The orbits of Venus, Earth, and Mars are known to subkilometer accuracy. Because of perturbations of the orbit of Mars by asteroids, frequent updates are needed to maintain the current accuracy into the future decade. Mercury's orbit is determined to an accuracy of several kilometers by radar ranging. The orbits of Jupiter and Saturn are determined to accuracies of tens of kilometers as a result of spacecraft tracking and modern ground-based astrometry. The orbits of Uranus, Neptune, and Pluto are not as well determined. Reprocessing of historical observations is expected to lead to improvements in their orbits in the next several years.

I. Introduction

The planetary and lunar ephemeris DE 421 is a significant advance over earlier ephemerides. Compared with DE 418, released in July 2007,[1] the DE 421 ephemeris includes additional data, especially range and very long baseline interferometry (VLBI) measurements of Mars spacecraft; range measurements to the European Space Agency's Venus Express spacecraft; and use of current best estimates of planetary masses in the integration process. The lunar orbit is more robust due to an expanded set of lunar geophysical solution parameters, seven additional months of laser ranging data, and complete convergence. DE 421 has been integrated over the time period 1900 to 2050.

While the lunar orbit in DE 421 is close to that in DE 418, it is a major improvement over the widely distributed DE 405 [1]. For DE 405, the lunar orbit was not fit in a way consistent with the other planets. Continuing the process used to develop DE 418, DE 421 is a combined fit of lunar laser ranging (LLR) and planetary measurements. The DE 421 model is more complete than for DE 418 and has been fully converged, so it is recommended for use by lunar missions.

---

* Guidance, Navigation, and Control Section.
† Tracking Systems and Applications Section.

[1] W. M. Folkner, E. M. Standish, J. G. Williams, and D. H. Boggs, "Planetary and Lunar Ephemeris DE 418," JPL Interoffice Memorandum 343R-07-005 (internal document), Jet Propulsion Laboratory, Pasadena, California, 2007.

The research described in this publication was carried out by the Jet Propulsion Laboratory, California Institute of Technology, under a contract with the National Aeronautics and Space Administration.

Also, DE 405 was created in 1995 before the Mars Pathfinder mission in 1997, so the Earth and Mars orbits were largely dependent on range measurements to the Viking landers from 1976 to 1982 augmented by radar range observations with an accuracy of about 1 km. The error in the Earth and Mars orbits in DE 405 is now known to be about 2 km, which was good accuracy in 1997 but much worse than the current subkilometer accuracy.

Because of perturbations of the orbit of Mars by asteroids, frequent updates are needed to maintain the current ephemeris accuracy into the future decade. The orbits of Earth and Mars are continually improved through measurements of spacecraft in orbit about Mars. DE 421 incorporates range data through the end of 2007. VLBI observations of Mars spacecraft were resumed in January 2006 to improve the Mars orbit accuracy for the Mars Science Laboratory project. VLBI data through December 2007 have been included in the DE 421 estimate. The Earth and Mars orbit accuracies are expected to be better than 300 m through 2008.

The Venus orbit accuracy has been significantly improved by inclusion of range measurements to the Venus Express spacecraft. Combined with VLBI measurements of Magellan, and one VLBI observation of Venus Express, the Venus orbit accuracy is now about 200 m.

The orbit of Mercury is currently determined by radar range observations. Since the last radar range point is in 1999, the estimated Mercury orbit has not changed significantly for the past decade. The current orbit accuracy is a few kilometers. Measurements of the Mercury Surface, Space Environment, Geochemistry, and Ranging (MESSENGER) spacecraft are expected to lead to a significant improvement over the next several years.

The orbits of Jupiter and Saturn are determined to accuracies of tens of kilometers using spacecraft tracking and modern ground-based astrometry. The orbit of Saturn is more accurate than that of Jupiter since the Cassini tracking data are more complete and more accurate than previous spacecraft tracking at Jupiter. The orbits of Uranus, Neptune, and Pluto are not as well determined. Reprocessing of historical observations is expected to lead to improvements in their orbits in the next several years.

Below we briefly summarize the dynamical modeling assumptions used in the development of DE 421 and the measurements used in its estimation.

II. Planetary Ephemeris Dynamical Modeling

The time coordinate for DE 421 is consistent with the metric used for integration. The coordinate time has been scaled such that at the location of Earth the coordinate time has no rate relative to atomic time. In a resolution adopted by the International Astronomical Union in 2006 (GA26.3), the timescale TDB (Temps Dynamique Barycentrique, or Barycentric Dynamical Time) was defined to be consistent with the JPL ephemeris time. The conversion from atomic time to coordinate time has been done using the formulation of [2], updated by [3], which is consistent, for planetary navigation accuracies, with the simpler approximation given in [4].

The axes of the ephemeris are oriented with respect to the International Celestial Reference Frame (ICRF). The Mars spacecraft VLBI measurements serve to tie the ephemeris to the ICRF with accuracy better than 1 milliarcsec (1 mas ≈ 5 nanorad) for the planets with accurate ranges.

For DE 421, the positions of the Moon and planets were integrated using an n-body parameterized post-Newtonian (PPN) metric [5,6,4]. The PPN parameters γ and β have been set to 1, their values in general relativity. Extended body effects for the Earth–Moon system are described elsewhere.[2] The oblateness of the Sun has been modeled with J_2 set to 2.0×10^{-7}. Along with the Earth/Moon mass ratio, the mass parameter GM for the Sun, which is by convention a fixed value in units of AU^3/day^2, was estimated in units of km^3/s^2 by solving for the AU in km in the development of DE 421. The mass parameter of the Earth–Moon system was held fixed to a previous LLR-only estimate. The mass parameters for the other planets (planetary systems for planets with natural satellites) were taken from published values derived from spacecraft tracking data. The mass parameters used for the Sun and planets are given in Table 1.

Table 1. Mass parameters of planetary bodies/systems used in DE 421.

Body/System	GM, km^3/s^{-2}	GM_{sun}/GM_{planet}	Reference
Mercury	22032.090000	6023597.400017	[7]
Venus	324858.592000	408523.718655	[8]
Earth	398600.436233	332946.048166	See text
Mars	42828.375214	3098703.590267	[9]
Jupiter	126712764.800000	1047.348625	Jacobson[3]
Saturn	37940585.200000	3497.901768	[10]
Uranus	5794548.600000	22902.981613	[11]
Neptune	6836535.000000	19412.237346	[12]
Pluto	977.000000	135836683.767599	Jacobson[4]
Sun	132712440040.944000	1	Estimated
Moon	4902.800076	27068703.185436	See text
Earth–Moon	403503.236310	328900.559150	LLR fit

The orbit of the Sun was not integrated in the same way as the orbits of the planets. Instead, the position and velocity of the Sun were derived at each integration time step to keep the solar system barycenter[5] at the center of the coordinate system.

The Newtonian effects of 67 "major" asteroids and 276 "minor" asteroids that introduce the largest perturbations on the orbit of Mars have been included in the integration of the planetary orbits in an iterative manner. The orbits of Ceres, Pallas, and Vesta were inte-

[2] J. G. Williams, D. H. Boggs, and W. M. Folkner, "DE421 Lunar Orbit, Physical Librations, and Surface Coordinates," JPL Interoffice Memorandum 335-JW, DB, WF-20080314-001 (internal document), Jet Propulsion Laboratory, Pasadena, California, March 14, 2008.

[3] R. A. Jacobson, personal communication, Principal Engineer, Guidance, Navigation, and Control Section, "Jovian satellite ephemeris JUP230," Jet Propulsion Laboratory, Pasadena, California, 2005.

[4] R. A. Jacobson, personal communication, Principal Engineer, Guidance, Navigation, and Control Section, "The orbits of the satellites of Pluto PLU017," 2007.

[5] F. B. Estabrook, "Derivation of Relativistic Lagrangian for n-body Equations Containing Relativity Parameters β and γ," JPL Interoffice Memorandum (internal document), Jet Propulsion Laboratory, Pasadena, California, 1971.

grated simultaneously, including mutual interactions, holding the orbits of the Sun and planets to those in DE 405. The orbits for the other asteroids were integrated individually under the gravitational forces from the Sun, planets, Ceres, Pallas, and Vesta, whose orbits were held fixed. The mass parameters of Ceres, Pallas, Vesta, and eight other asteroids were then estimated in fitting the DE 421 data. The mass parameters of the remaining 56 "major" asteroids were held at assumed nominal values. The mass parameters of the major asteroids are given in Appendix A. The minor asteroids were divided into three taxonomic types (classes). The volume of each minor asteroid was based on a nominal radius and the density of each of the three types of asteroids was estimated. The estimated densities and the radii assumed for the minor asteroids are given in Appendix A.

The selection of which asteroid mass parameters to estimate was based on an empirical process to see which set produced a reasonably accurate prediction of the Earth–Mars range over 1 year. For example, Figure 1 shows Mars Odyssey range residuals relative to DE 418, which was fit to range data through the end of 2006. DE 418 is seen to predict the range to Mars 1 year into the future with an accuracy of about 15 m. Similarly, DE 421 is expected to predict the Earth–Mars range to about 15 m through the end of 2008. (The error in the plane-of-sky position of Mars relative to Earth through the end of 2008 is about 300 m.) This was relevant for navigation of the Phoenix spacecraft, which arrived at Mars in May 2008. The estimated mass parameters of the selected asteroids and estimated asteroid class densities are not necessarily the best possible values for other purposes.

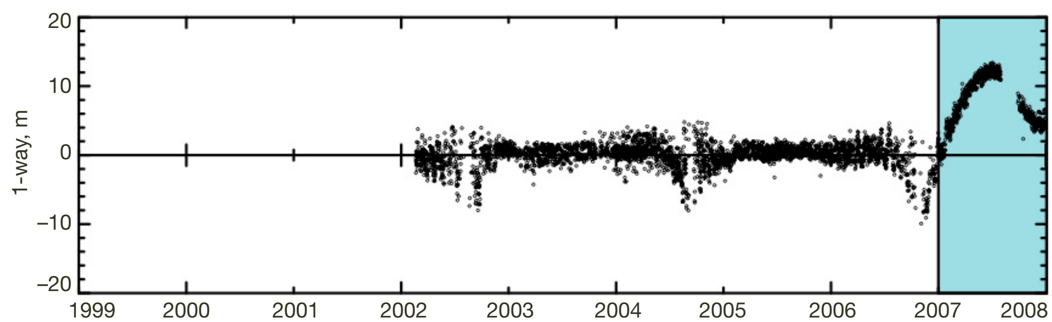

Figure 1. Mars Odyssey spacecraft range measurement residuals with respect to planetary ephemeris DE 418. DE 418 was fit to range measurements through the end of 2006. The range residuals for data in 2007 (in shaded area) are less than 15 m and indicate the ephemeris prediction accuracy.

III. Measurement Set

Rather than try to fit all available planetary observations, the data used for DE 421 were preferentially selected for the best accuracy and (for angular data) accuracy of ties to the ICRF. The measurements are summarized in Table 2 and Table 3. Plots of the residuals for all data are included in Appendix B. The data for each planet contain primary data that have the most strength for determining the orbit and, for some planets, secondary data that are included in the fit at their nominal weight but do not affect the orbit significantly.

Table 2. Summary of data used to estimate orbits of the Moon, inner planets, and Jupiter. Data with relatively little contribution to the estimated orbits are indicated in italics.

Object	Measurement	Type	Observatory	Span	No. Meas.
Moon	LLR	Range	McDonald 2.7 m	1970–1985	3451
			MLRS/Saddle	1984–1988	275
			MLRS/Mt. Fowlkes	1988–2007	2746
			Haleakala	1984–1990	694
			CERGA	1984–2005	9177
			Matera	2004	11
			Apache Pt.	2006–2007	247
Mercury	Radar	Range	Arecibo	1967–1982	242
			Goldstone	1972–1997	283
			Haystack	1966–1971	217
			Eupatoria	1980–1995	75
	Radar	Closure	Goldstone	1989–1997	40
	Spacecraft	Range	Mariner 10	1974–1975	2
Venus	Spacecraft	Range	VEX	2006–2007	14304
	Spacecraft	VLBI	VEX	2007	1
	Spacecraft	VLBI	MGN	1990–1994	18
	Spacecraft	3-D	Cassini	1998–1999	2
	Radar	*Range*	*Arecibo*	*1967–1970*	*227*
			Goldstone	*1970–1990*	*512*
			Haystack	*1966–1971*	*229*
			Millstone	*1964–1967*	*101*
			Eupatoria	*1962–1995*	*1134*
Mars	Spacecraft	Range	Viking L1	1976–1982	1178
			Viking L2	1976–1977	80
			Pathfinder	1997	90
			MGS	1999–2006	164781
			Odyssey	2002–2007	251999
			MEX	2005–2007	63133
			MRO	2006–2007	7972
	Spacecraft	VLBI	MGS	2001–2003	14
			ODY	2002–2007	66
			MRO	2006–2007	14
Jupiter	Spacecraft	3-D	Pioneer 10	1973	1
			Pioneer 11	1974	1
			Voyager 1	1979	1
			Voyager 2	1979	1
			Ulysses	1992	1
			Cassini	2000	1
	CCD	RA/Dec	USNOFS	1998–2007	2533
	Spacecraft	VLBI	Galileo	1996–1997	24
	Transit	*RA/Dec*	*Washington*	*1914–1994*	*2053*
			Herstmonceux	*1958–1982*	*468*
			La Palma	*1992–1997*	*658*
			Tokyo	*1986–1988*	*98*
			El Leoncito	*1998*	*11*

MLRS – McDonald Laser Ranging Station; CERGA – Centre d'Etudes et de Recherches Géodynamiques et Astronomiques; VEX – Venus Explorer; MGN – Magellan; Viking L1 – Lander 1; Viking L2 – Lander 2; MGS – Mars Global Surveyor; MRO – Mars Reconnaissance Orbiter; ODY – Mars Odyssey; USNOFS – U. S. Naval Observatory Flagstaff Station

Table 3. Summary of data used to estimate orbits of Saturn, Uranus, Neptune, and Pluto. Data with relatively little contribution to the estimated orbits are indicated in italics.

Object	Measurement	Type	Observatory	Span	No. Meas.
Saturn	Spacecraft	3-D	Pioneer 11	1979	1
			Voyager 1	1980	1
			Voyager 2	1981	1
			Cassini	2004–2006	31
	CCD	RA/Dec	USNOFS	1998–2007	3153
			TMO	2002–2005	778
	Transit	*RA/Dec*	*Bordeaux*	*1987–1993*	*119*
			Washington	*1913–1982*	*1422*
			Herstmonceux	*1958–1982*	*405*
			La Palma	*1992–1997*	*730*
			Tokyo	*1986–1988*	*62*
			El Leoncito	*1998*	*18*
Uranus	Spacecraft	3-D	Voyager 2	1986	1
	CCD	RA/Dec	USNOFS	1998–2007	1612
			TMO	1998–2007	347
	Transit	RA/Dec	Bordeaux	1985–1993	165
			Washington	1914–1993	2043
			Herstmonceux	1957–1981	353
			La Palma	1984–1997	1030
			Tokyo	1986–1988	44
			El Leoncito	1997–1998	8
Neptune	Spacecraft	3-D	Voyager 2	1989	1
	CCD	RA/Dec	USNOFS	1998–2007	1588
			TMO	2001–2007	267
	Transit	RA/Dec	Bordeaux	1985–1993	348
			Washington	1913–1993	1838
			Herstmonceux	1958–1981	316
			La Palma	1984–1998	1106
			Tokyo	1986–1988	59
			El Leoncito	1998–1999	11
Pluto	CCD	RA/Dec	USNOFS	1998–2007	852
			TMO	2001–2007	118
	Photo	RA/Dec	Misc.	1914–1958	42
			Palomar	1963–1965	8
			Pulkovo	1930–1992	53
			Bord/Valin	1995–2001	97
			Asiago	1969–1989	193
			Copenhagen	1975–1978	15
			Lick	1980–1985	11
			Torino	1973–1982	37
	Transit	*RA/Dec*	*La Palma*	*1989–1998*	*380*
			El Leoncito	*1999*	*33*

USNOFS – U. S. Naval Observatory Flagstaff Station; TMO – Table Mountain Observatory

LLR, spacecraft ranging, and radar ranging are all very accurate and independent of reference frame. VLBI observations of spacecraft in orbit about Venus, Mars, Jupiter, and Saturn relative to extragalactic radio sources defining the ICRF tie the planetary ephemeris to the ICRF.

Analysis of spacecraft range and Doppler observations taken as spacecraft fly by planets can give right ascension (RA) and declination (Dec) with accuracy somewhat less than the VLBI observations. These right ascension and declination determinations are important in refining the orbits of Jupiter and Saturn. The accuracy of spacecraft plane-of-sky determinations is very much a function of time. The earliest planetary encounters relied on 2-GHz (S-band) radio systems with range and Doppler measurement accuracy very sensitive to electrons in the solar plasma. Later spacecraft observations (e.g., after 1990) used 8-GHz (X-band) radio systems that were much less affected by solar plasma. Early spacecraft encounter data were processed with reference frame models not well linked to the current ICRF, and often saw discrepancies between range and Doppler data. Data from most encounters have since been reprocessed with modern reference frame models so the determined plane-of-sky positions are consistent with the ICRF. For each encounter, a single vector for range, RA, and Dec was generated. For Cassini, a vector was generated for each orbit about Saturn.

Astrometric observations of the planets in the past have suffered from the difficulty in establishing an accurate celestial reference frame. Since the release of the Hipparcos star catalog, and the development of techniques for using charge-coupled device (CCD) instruments, astrometric accuracies are approaching spacecraft VLBI accuracies. However, these observations only cover a fraction of the orbital periods of the outer planets. Since the orbits of Jupiter and Saturn are well determined from spacecraft data, the limited time span of modern data mainly affects the orbital uncertainties of Uranus, Neptune, and Pluto. The Pluto data set was discussed in detail in relation to the ephemeris DE 418.[6] For the orbit of Pluto in DE 421, we followed the same approach used for DE 418, with two more months of observations. For Uranus and Neptune, the assessment of older data sets is not as complete as for Pluto so relatively few data have been included. These orbits are reasonably accurate for the current times due to modern astrometry and knowledge from the Voyager encounters. The Uranus and Neptune data sets will be expanded in a future ephemeris.

Most of the data used are not published but communicated to the authors electronically.[7] LLR data are posted by the International Laser Ranging Service [13].[8] Mariner 10 range to Mercury was reported by [7]. Goldstone radar range to Mercury is from [14]. Radar ranges to Mercury and Venus from Eupatoria are from [15].[9] Astrometry data from the U. S. Naval Observatory are from [16].[10] Older observations of Pluto are taken from the literature — see [17–20, [21], [22], [23], [24–26], [27], [28], [29], [30–31]. Other data were obtained via personal communications.

---

[6] Folkner et al., 2007, op cit.

[7] Most data are available at the website http://iau-comm4.jpl.nasa.gov/plan-eph-data/ or by request from the authors.

[8] http://ilrs.gsfc.nasa.gov/

[9] http://www.ipa.nw.ru/PAGE/DEPFUND/LEA/ENG/rrr.html

[10] http://www.nofs.navy.mil/data/plansat.html

IV. Availability

The DE 421 ephemeris may be downloaded in an ASCII version from this site — ftp://ssd.jpl.nasa.gov/pub/eph/planets/ascii/de421

The complete set of input parameters for the solar system integration is part of the file. The SPICE[11] kernal version of DE 421 is available at this site — ftp://ssd.jpl.nasa.gov/pub/eph/planets/bsp

Acknowledgments

The planetary ephemeris accuracy is limited by the accuracy of measurements to which it is fit. The present ephemeris improvements are due to contributed data from many people, including Jim Border for the spacecraft VLBI measurements, Don Han for files used to reduce some of the VLBI measurements, Alex Konopliv for reduced NASA Mars spacecraft ranging measurements, Hugh Harris and Alice Monet at the U. S. Naval Observatory in Flagstaff for observations of the outer planets, Trevor Morely and staff at the European Space Operations Center for Venus Express and Mars Express range measurements, Bob Jacobson for reduction of Voyager, Pioneer, and Cassini spacecraft tracking data, and Bill Owen for observations of the outer planets from Table Mountain Observatory. Modern lunar laser range quality and quantity are the products of the personnel of the McDonald Observatory in Texas, Apache Point Observatory in New Mexico, Observatoire de la Côte d'Azur in France, and Haleakala Observatory in Hawai'i. This work is also greatly dependent on the work of M. Standish, who advised us on aspects of the ephemeris development.

References

[1] E. M. Standish, X. X. Newhall, J. G. Williams, and W. M. Folkner, *JPL Planetary and Lunar Ephemerides*, CD-ROM published by Willmann-Bell, Inc., Richmond, Virginia, 1997.

[2] L. Fairhead and P. Bretagnon, "An Analytical Formula for the Time Transformation TB-TT," *Astronomy and Astrophysics*, vol. 229, pp. 240–247, 1990.

[3] T. Fukushima and A. A. Irwin, "A Numerical Time Ephemeris of the Earth," *Astronomy and Astrophysics*, vol. 348, pp. 642–652, 1999.

[4] T. D. Moyer, *Formulation for Observed and Computed Values of Deep Space Network Data Types for Navigation*, Monograph 2, Deep Space Communications and Navigation Series, Jet Propulsion Laboratory, Pasadena, California, 2000.

[5] C. M. Will and K. Nordtvedt, "Conservation Laws and Preferred Frames in Relativistic Gravity: I. Preferred-Frame Theories and an Extended PPN Formalism," *Astrophysical Journal*, vol. 177, pp. 757–774, 1972.

[11] For SPICE information, documentation, and toolkit — http://naif.jpl.nasa.gov

[6] C. M. Will, *Theory and Experiment in Gravitational Physics*, Cambridge University Press, 1981.

[7] J. D Anderson, G. Colombo, P. B. Esposito, E. L. Lau, and G. B. Trager, "The Mass, Gravity Field, and Ephemeris of Mercury," *Icarus*, vol. 71, pp. 337–349, 1987.

[8] A. S. Konopliv, W. B. Banerdt, and W. L. Sjogren, "Venus Gravity: 180th Degree and Order Model," *Icarus*, vol. 139, pp. 3–18, 1999.

[9] A. S. Konopliv, C. F. Yoder, E. M. Standish, D. Yuan, and W. L. Sjogren, "A Global Solution for the Mars Static and Seasonal Gravity, Mars Orientation, Phobos and Deimos Masses, and Mars Ephemeris," *Icarus*, vol. 182, pp. 23–50, 2006.

[10] R. A. Jacobson, P. G. Antreasian, J. J. Bordi, K. E. Criddle, R. Ionasescu, J. B. Jones, R. A. Mackenzie, F. J. Pelletier, W. M. Owen Jr., D. C. Roth, and J. R. Stauch, "The Gravity Field of the Saturnian System from Satellite Observations and Spacecraft Tracking Data," *Astronomical Journal*, vol. 132, pp. 2520–2526, 2006.

[11] R. A. Jacobson, J. K. Campbell, A. H. Taylor, and S. P. Synnott, "The Masses of Uranus and Its Major Satellites from Voyager Tracking Data and Earth-Based Uranus Satellite Data," *Astronomical Journal*, vol. 103, pp. 2068–2078, 1992.

[12] R. A. Jacobson, J. E. Riedel, and A. H. Taylor, "The Orbits of Triton and Nereid from Spacecraft and Earth-Based Observations," *Astronomy and Astrophysics*, vol. 247, pp. 565–575, 1991.

[13] M. R. Pearlman, J. J. Degnan, and J. M. Bosworth, "The International Laser Ranging Service," *Advances in Space Research*, vol. 30, no. 2, pp. 135–143, July 2002, DOI:10.1016/S0273-1177(02)00277-6.

[14] R. F. Jurgens, F. Rojas, M. A. Slade, E. M. Standish, and J. F. Chandler, "Mercury Radar Ranging Data from 1987 to 1997," *Astronomical Journal*, vol. 116, pp. 486–488, 1998.

[15] V. A. Kotelnikov, Y. N. Alexandrov, R. A. Andreev, A. S. Vyshlov, V. M. Dubrovin, A. L. Zajtsev, S. P. Ignatov, V. I. Kaevitser, A. N. Kozlov, A. A. Krymov, E. P. Molotov, G. M. Petrov, O. N. Rzhiga, A. T. Tagaevskij, A. F. Khasyanov, A. M. Shakhovskoj, and S. A. Shchetinnikov, "Radar Observations of Planets," *Astronomicheskii Zhurnal*, vol. 60, no. 3, 1983.

[16] R. C. Stone, D. G. Monet, A. K. B. Monet, F. H. Harris, H. D. Ables, C. C. Dahn, B. Canzian, H. H. Guetter, H. C. Harris, A. A. Henden, S. E. Levine, C. B. Luginbuhl, J. A. Munn, J. R. Pier, F. J. Vrba, and R. L. Walker, "Upgrades to the Flagstaff Astrometric Scanning Transit Telescope: A Fully Automated Telescope for Astrometry," *Astronomical Journal*, vol. 126, pp. 2060–2080, 2003.

[17] C. Barbieri, M. Capaccioli, R. Ganz, and G. Pinto, "Accurate Positions of the Planet Pluto in the Years 1969–1970," *Astronomical Journal*, vol. 77, pp. 521–522, 1972.

[18] C. Barbieri, M. Capaccioli, and G. Pinto, "Accurate Positions of the Planet Pluto in the Years 1971–1974," *Astronomical Journal*, vol. 80, pp. 412–414, 1975.

[19] C. Barbieri, L. Pinocchio, M. Capacciloi, G. Pinto, and A. A. Schoenmaker, "Accurate Positions of the Planet Pluto from 1974 to 1978," *Astronomical Journal*, vol. 84, pp. 1890–1893, 1979.

[20] C. Barbieri, L. Benacchio, M. Capacciloi, and A. G. Gemmo, "Accurate Positions of the Planet Pluto from 1979 to 1987," *Astronomical Journal*, vol. 96, pp. 396–399, 1988.

[21] C. J. Cohen, E. C. Hubbard, and C. Oesterwinter, "New Orbit for Pluto and Analysis of Differential Corrections," *Astronomical Journal*, vol. 8, pp. 973–988, 1967.

[22] K. S. Jensen, "Accurate Astrometric Positions of Pluto, 1975–1978," *Astronomy and Astrophysics Supplement*, vol. 36, pp. 395–398, 1979.

[23] A. G. Gemmo and C. Barbieri, "Astrometry of Pluto from 1969 to 1989," *Icarus*, vol. 108, pp. 174–179, 1994.

[24] A. R. Klemola and E. A. Harlan, "Astrometric Observations of the Outer Planets and Minor Planets: 1980–1982," *Astronomical Journal*, vol. 87, pp. 1242–1243, 1982.

[25] A. R. Klemola and E. A. Harlan, "Astrometric Observations of the Outer Planets and Minor Planets: 1982–1983," *Astronomical Journal*, vol. 89, pp. 879–881, 1984.

[26] A. R. Klemola and E. A. Harlan, "Astrometric Observations of the Outer Planets and Minor Planets: 1984–1985," *Astronomical Journal*, vol. 92, pp. 195–198, 1986.

[27] M. Rapaport, R. Teixeira, J. F. Le Campion, C. Ducourant, J. I. B. Camargo, and P. Benevides-Soares, "Astrometry of Pluto and Saturn with the CCD Meridian Instruments of Bordeaux and Valinhos," *Astronomy and Astrophysics*, vol. 383, pp. 1054–1061, 2002.

[28] V. P. Rylkov, V. V. Vityazev, and A. A. Dementieva, "Pluto: An Analysis of Photographic Positions Obtained with the Pulkovo Normal Astrograph in 1930–1992," *Astronomical and Astrophysical Transactions*, vol. 6, pp. 251–281, 1995.

[29] Sh. G. Sharaf and N. A. Budnikova, "Theory of the Motion of the Planet Pluto," *Transactions of the Institute of Theoretical Astronomy*, vol. 10, pp. 1–173, 1964, published as NASA Technical Translation F-491, 1969.

[30] V. Zappala, G. de Sanctis, and W. Ferreri, "Astrometric Observations of Pluto from 1973 to 1979," *Astronomy and Astrophysics Supplement*, vol. 41, pp. 29–31, 1980.

[31] V. Zappala, G. de Sanctis, and W. Ferreri, "Astrometric Positions of Pluto from 1980 to 1982," *Astronomy and Astrophysics Supplement*, vol. 51, pp. 385–387, 1983.

Appendix A

Asteroid Parameters

Table A-1. Parameters of "major" asteroids — r = radius, GM = mass, ρ = density.

ID	Name	r, km	Type	GM, km^3/s^2	ρ, gm/cm^3	ID	Name	r, km	Type	GM, km^3/s^2	ρ, gm/cm^3
1	Ceres	474.0	G	62.178	2.1	63	Ausonia	51.6	S	0.102	2.7
2	Pallas	266.0	B	13.402	2.5	65	Cybele	118.6	C	0.694	1.5
3	Juno	117.0	Sk	1.536	3.4	69	Hesperia	69.1	M	0.414	4.5
4	Vesta	265.0	V	17.630	3.4	78	Diana	60.3	C	0.085	1.4
5	Astraea	59.5	S	0.159	2.7	94	Aurora	102.4	C	0.414	1.4
6	Hebe	92.6	S	0.605	2.7	97	Klotho	41.4	M	0.089	4.5
7	Iris	99.9	S	0.796	2.9	98	Ianthe	52.2	C	0.055	1.4
8	Flora	67.9	S	0.236	2.7	105	Artemis	59.5	C	0.088	1.5
9	Metis	95.0	S	0.567	2.4	111	Ate	67.3	C	0.116	1.4
10	Hygiea	203.6	C	5.364	2.3	135	Hertha	39.6	M	0.078	4.5
11	Parthenope	77.7	S	0.356	2.7	139	Juewa	78.3	C	0.188	1.4
13	Egeria	103.8	C	0.412	1.3	145	Adeona	75.6	C	0.151	1.3
14	Irene	76.0	S	0.348	2.8	187	Lamberta	65.6	C	0.105	1.3
15	Eunomia	127.7	S	1.638	2.8	192	Nausikaa	51.6	S	0.107	2.8
16	Psyche	126.6	M	2.233	3.9	194	Prokne	84.2	C	0.182	1.1
18	Melpomene	70.3	S	0.267	2.7	216	Kleopatra	62.0	M	0.299	4.5
19	Fortuna	100.0	Ch	0.463	1.7	230	Athamantis	54.5	S	0.126	2.8
20	Massalia	72.8	S	0.291	2.7	324	Bamberga	114.5	CP	0.661	1.6
21	Lutetia	47.9	M	0.139	4.5	337	Devosa	29.6	M	0.033	4.5
22	Kalliope	90.5	M	0.491	2.4	344	Desiderata	66.1	C	0.114	1.4
23	Thalia	53.8	S	0.129	3.0	354	Eleonora	77.6	Sl	0.327	2.5
24	Themis	99.0	C	0.403	1.5	372	Palma	94.3	C	0.355	1.5
25	Phocaea	37.6	S	0.040	2.7	405	Thia	62.5	C	0.092	1.4
27	Euterpe	48.0	S	0.084	2.7	409	Aspasia	80.8	C	0.216	1.5
28	Bellona	60.5	S	0.165	2.7	419	Aurelia	64.5	C	0.102	1.4
29	Amphitrite	106.1	S	0.906	2.7	451	Patientia	112.5	C	0.610	1.5
30	Urania	49.8	S	0.095	2.7	488	Kreusa	75.1	C	0.164	1.4
31	Euphrosyne	128.0	C	1.139	1.9	511	Davida	163.0	C	1.638	1.4
41	Daphne	87.0	Ch	0.527	2.9	532	Herculina	111.1	S	0.886	2.3
42	Isis	50.1	S	0.092	2.6	554	Peraga	47.9	C	0.044	1.4
45	Eugenia	107.3	C	0.397	1.2	654	Zelinda	63.7	Ch	0.090	1.2
51	Nemausa	73.9	C	0.144	1.3	704	Interamnia	158.3	C	2.464	2.2
52	Europa	151.3	C	1.354	1.4	747	Winchester	85.9	C	0.196	1.1
60	Echo	30.1	S	0.021	2.7						

Table A-2. Estimated densities ρ in gm/cm^3 of "minor" asteroids.

Type	ρ
C	1.093
S	3.452
M	4.221

Table A-3. Parameters of "minor" asteroids — r = radius.

ID	Name	Type	r, km	ID	Name	Type	r, km	ID	Name	Type	r, km
12	Victoria	S	56.4	92	Undina	M	63.2	171	Ophelia	C	58.3
17	Thetis	S	45.0	93	Minerva	C	70.5	172	Baucis	S	31.2
26	Proserpina	S	47.5	95	Arethusa	C	68.0	173	Ino	C	77.1
32	Pomona	S	40.4	96	Aegle	C	85.0	175	Andromache	C	50.5
34	Circe	C	56.8	99	Dike	C	36.0	176	Iduna	C	60.5
35	Leukothea	C	51.6	100	Hekate	S	44.3	177	Irma	C	36.6
36	Atalante	C	52.8	102	Miriam	C	41.5	181	Eucharis	S	53.0
37	Fides	S	54.2	103	Hera	S	45.6	185	Eunike	C	78.8
38	Leda	C	58.0	104	Klymene	C	61.8	191	Kolga	C	50.5
39	Laetitia	S	74.8	106	Dione	C	73.3	195	Eurykleia	C	42.9
40	Harmonia	S	53.8	107	Camilla	C	111.3	196	Philomela	S	68.2
43	Ariadne	S	32.9	109	Felicitas	C	44.7	198	Ampella	S	28.6
44	Nysa	S	35.3	110	Lydia	M	43.0	200	Dynamene	C	64.2
46	Hestia	C	62.1	112	Iphigenia	C	36.1	201	Penelope	M	34.2
47	Aglaja	C	63.5	113	Amalthea	S	23.1	203	Pompeja	C	58.1
48	Doris	C	110.9	114	Kassandra	C	49.8	205	Martha	C	40.5
49	Pales	C	74.9	115	Thyra	S	39.9	206	Hersilia	C	56.5
50	Virginia	C	49.9	117	Lomia	C	74.4	209	Dido	C	80.0
53	Kalypso	C	57.7	118	Peitho	S	20.9	210	Isabella	C	43.3
54	Alexandra	C	82.9	120	Lachesis	C	87.1	211	Isolda	C	71.6
56	Melete	C	56.6	121	Hermione	C	104.5	212	Medea	C	68.1
57	Mnemosyne	S	56.3	124	Alkeste	S	38.2	213	Lilaea	C	41.5
58	Concordia	C	46.7	127	Johanna	C	61.0	221	Eos	S	51.9
59	Elpis	C	82.4	128	Nemesis	C	94.1	223	Rosa	C	43.8
62	Erato	C	47.7	129	Antigone	M	56.5	224	Oceana	M	30.9
68	Leto	S	61.3	130	Elektra	C	91.1	225	Henrietta	C	60.2
70	Panopaea	C	61.1	132	Aethra	M	21.3	227	Philosophia	C	43.7
71	Niobe	S	41.7	134	Sophrosyne	C	54.0	233	Asterope	C	51.4
72	Feronia	C	43.1	137	Meliboea	C	72.7	236	Honoria	S	43.1
74	Galatea	C	59.4	140	Siwa	C	54.9	238	Hypatia	C	74.2
75	Eurydike	M	27.8	141	Lumen	C	65.5	240	Vanadis	C	52.0
76	Freia	C	91.8	143	Adria	C	45.0	241	Germania	C	84.5
77	Frigga	M	34.6	144	Vibilia	C	70.9	247	Eukrate	C	67.2
79	Eurynome	S	33.2	146	Lucina	C	66.1	250	Bettina	M	39.9
80	Sappho	S	39.2	147	Protogeneia	C	66.5	259	Aletheia	C	89.3
81	Terpsichore	C	59.5	148	Gallia	S	48.9	266	Aline	C	54.5
82	Alkmene	S	30.5	150	Nuwa	C	75.6	268	Adorea	C	69.9
83	Beatrix	C	40.7	154	Bertha	C	92.5	275	Sapientia	C	51.5
84	Klio	C	39.6	156	Xanthippe	C	60.5	276	Adelheid	C	60.8
85	Io	C	77.4	159	Aemilia	C	62.5	283	Emma	C	74.0
86	Semele	C	60.3	160	Una	C	40.6	287	Nephthys	S	33.8
87	Sylvia	C	130.5	162	Laurentia	C	49.6	303	Josephina	C	49.6
88	Thisbe	C	116.0	163	Erigone	C	36.3	304	Olga	C	33.9
89	Julia	S	75.7	164	Eva	C	52.5	308	Polyxo	C	70.3
90	Antiope	C	60.0	165	Loreley	C	77.6	313	Chaldaea	C	48.2
91	Aegina	C	54.9	168	Sibylla	C	74.2	322	Phaeo	M	35.4

Table A-3 continues on the next page

Table A-3 (continued). Parameters of "minor" asteroids — r = radius.

ID	Name	Type	r, km	ID	Name	Type	r, km	ID	Name	Type	r, km
326	Tamara	C	46.5	445	Edna	C	43.6	667	Denise	C	40.6
328	Gudrun	S	61.5	449	Hamburga	C	42.8	674	Rachele	S	48.7
329	Svea	C	38.9	454	Mathesis	C	40.8	675	Ludmilla	S	38.0
334	Chicago	C	77.9	455	Bruchsalia	C	42.2	680	Genoveva	C	42.0
335	Roberta	C	44.5	464	Megaira	C	37.0	683	Lanzia	C	41.0
336	Lacadiera	C	34.6	465	Alekto	C	36.7	690	Wratislavia	C	67.5
338	Budrosa	M	31.6	466	Tisiphone	C	57.8	691	Lehigh	C	43.8
345	Tercidina	C	47.1	469	Argentina	C	62.8	694	Ekard	C	45.4
346	Hermentaria	S	53.3	471	Papagena	S	67.1	696	Leonora	C	37.9
347	Pariana	M	25.6	476	Hedwig	C	58.4	702	Alauda	C	97.4
349	Dembowska	S	69.9	481	Emita	C	116.0	705	Erminia	C	67.1
350	Ornamenta	C	59.2	485	Genua	S	31.9	709	Fringilla	C	48.3
356	Liguria	C	65.7	489	Comacina	C	69.7	712	Boliviana	C	63.8
357	Ninina	C	53.0	490	Veritas	C	57.8	713	Luscinia	C	52.8
358	Apollonia	C	44.7	491	Carina	C	48.7	735	Marghanna	C	37.2
360	Carlova	C	57.9	498	Tokio	C	41.4	739	Mandeville	C	53.7
362	Havnia	C	49.0	503	Evelyn	C	40.8	740	Cantabia	C	45.4
363	Padua	C	48.5	505	Cava	C	57.5	751	Faina	C	55.3
365	Corduba	C	53.0	506	Marion	C	53.0	752	Sulamitis	M	31.4
366	Vincentina	C	46.9	508	Princetonia	C	71.2	760	Massinga	S	35.6
369	Aeria	M	30.0	514	Armida	C	53.1	762	Pulcova	C	68.5
373	Melusina	C	47.9	516	Amherstia	M	36.5	769	Tatjana	C	53.2
375	Ursula	C	108.0	517	Edith	M	45.6	772	Tanete	C	58.8
377	Campania	C	45.5	521	Brixia	C	57.8	773	Irmintraud	C	47.9
381	Myrrha	C	60.3	535	Montague	C	37.2	776	Berbericia	C	75.6
385	Ilmatar	S	45.8	536	Merapi	C	75.7	778	Theobalda	C	32.0
386	Siegena	C	82.5	545	Messalina	C	55.6	780	Armenia	C	47.2
387	Aquitania	S	50.3	547	Praxedis	M	34.8	784	Pickeringia	C	44.7
388	Charybdis	C	57.1	566	Stereoskopia	C	84.1	786	Bredichina	C	45.8
389	Industria	S	39.5	568	Cheruskia	C	43.5	788	Hohensteina	C	51.8
393	Lampetia	C	48.4	569	Misa	C	36.5	790	Pretoria	C	85.2
404	Arsinoe	C	48.8	584	Semiramis	S	27.0	791	Ani	C	51.8
407	Arachne	C	47.5	585	Bilkis	C	29.1	804	Hispania	C	78.6
410	Chloris	C	61.8	591	Irmgard	M	25.9	814	Tauris	C	54.8
412	Elisabetha	C	45.5	593	Titania	C	37.7	849	Ara	M	30.9
415	Palatia	C	38.2	595	Polyxena	C	54.5	895	Helio	C	71.0
416	Vaticana	S	42.7	596	Scheila	C	56.7	909	Ulla	C	58.2
420	Bertholda	C	70.6	598	Octavia	C	36.2	914	Palisana	C	38.3
423	Diotima	C	104.4	599	Luisa	S	32.4	980	Anacostia	S	43.1
424	Gratia	C	43.6	602	Marianna	C	62.4	1015	Christa	C	48.5
426	Hippo	C	63.5	604	Tekmessa	M	32.6	1021	Flammario	C	49.7
431	Nephele	C	47.5	618	Elfriede	C	60.1	1036	Ganymed	S	15.8
432	Pythia	S	23.4	623	Chimaera	C	22.1	1093	Freda	C	58.4
433	Eros	S	9.7	626	Notburga	C	50.4	1107	Lictoria	M	39.6
442	Eichsfeldia	C	32.9	635	Vundtia	C	49.1	1171	Rusthawelia	C	35.1
444	Gyptis	C	79.8	663	Gerlinde	C	50.4	1467	Mashona	C	112.0

Appendix B

Measurement Residual Plots

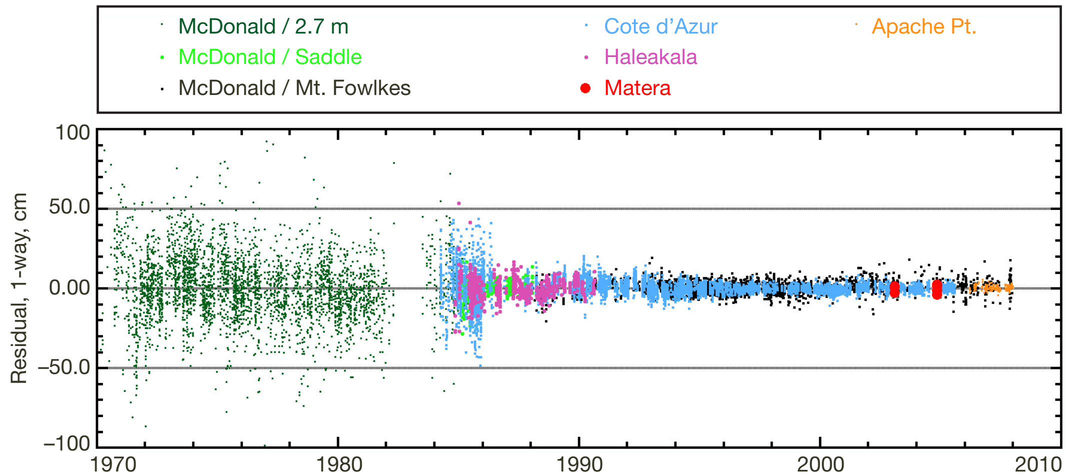

Figure B-1. Lunar laser ranging residuals.

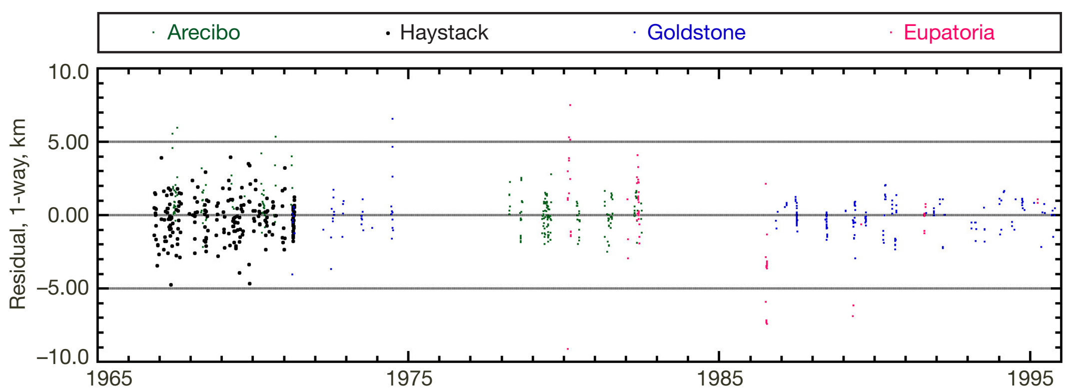

Figure B-2. Mercury radar range residuals.

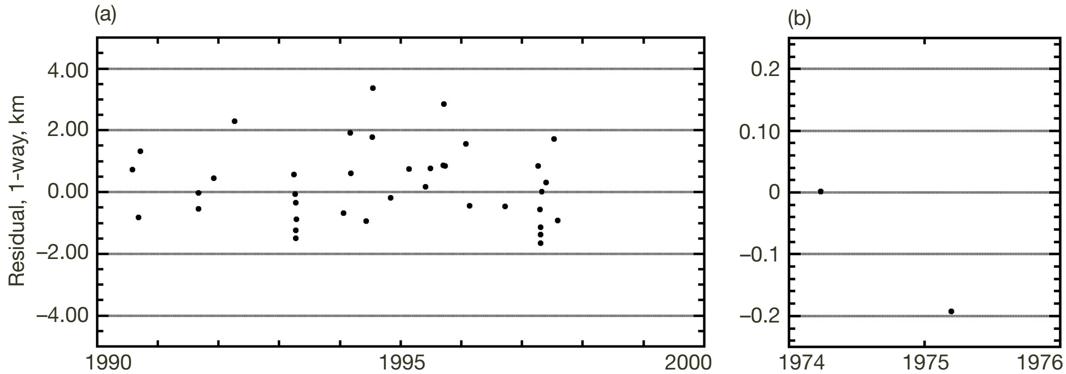

Figure B-3. (a) Mercury radar closure residuals; (b) Mariner 10 range residuals at Mercury.

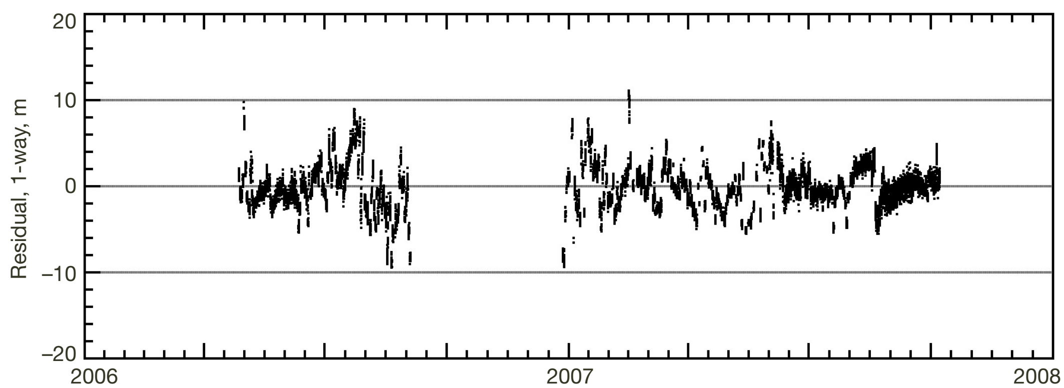

Figure B-4. Venus Express range residuals.

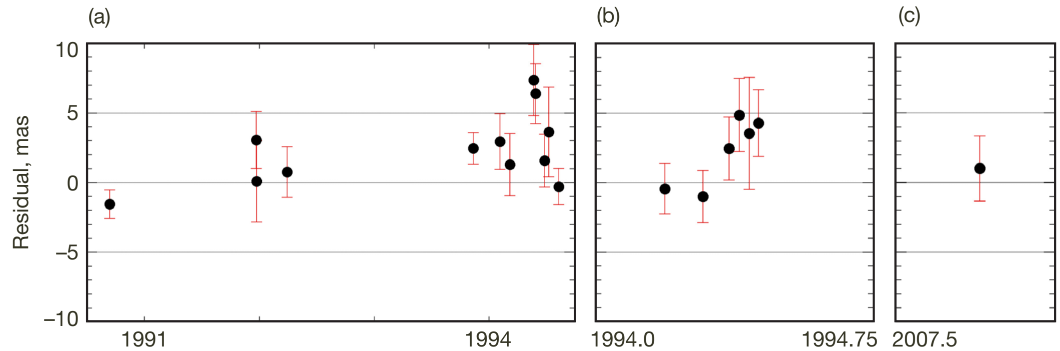

Figure B-5. Venus spacecraft VLBI residuals: (a) Magellan from Goldstone–Canberra baseline; (b) Magellan from Goldstone–Madrid baseline; (c) Venus Express from Goldstone–Madrid baseline.

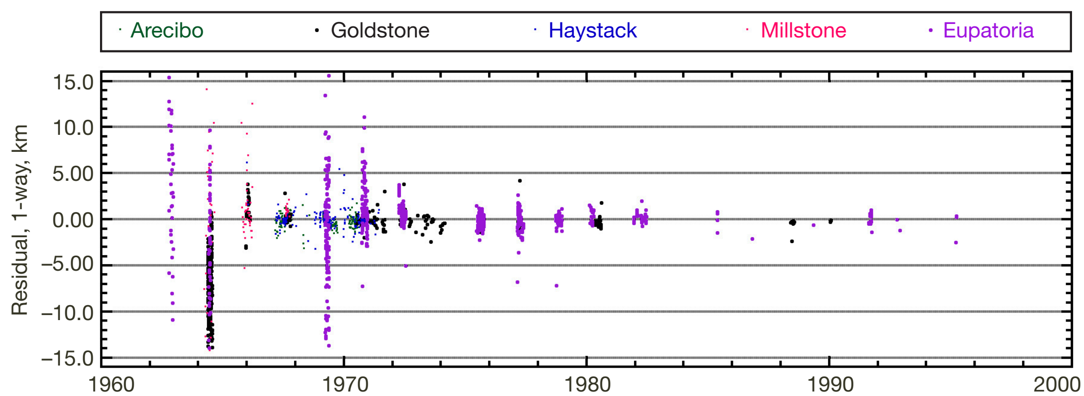

Figure B-6. Venus radar range residuals.

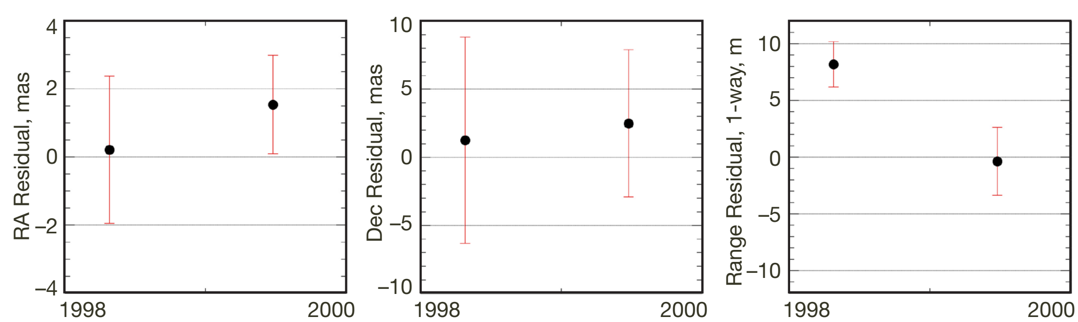

Figure B-7. Residuals for Cassini encounters at Venus.

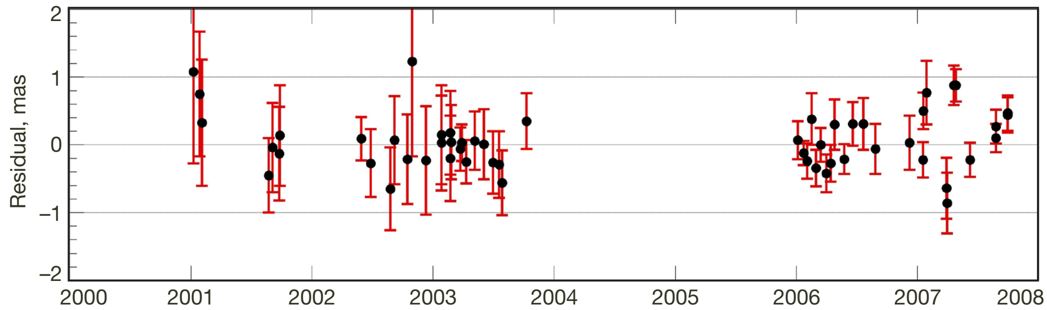

Figure B-8. Residuals for Mars spacecraft VLBI on Goldstone–Canberra baseline.

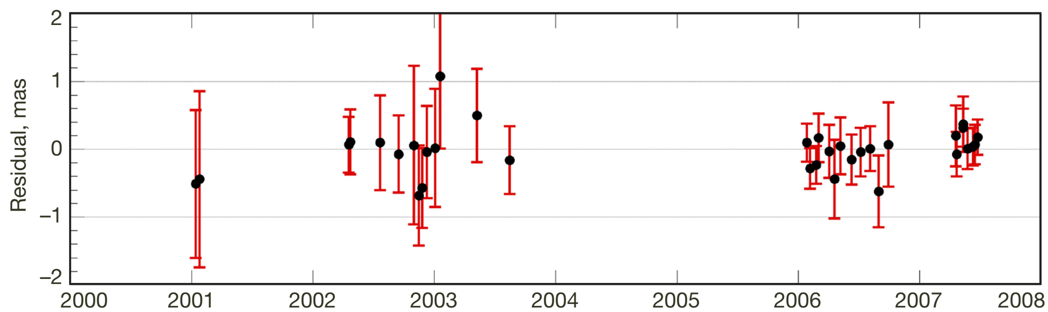

Figure B-9. Residuals for Mars spacecraft VLBI on Goldstone–Madrid baseline.

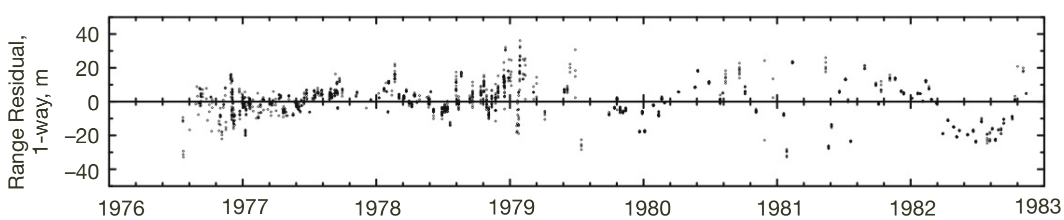

Figure B-10. Viking Lander range residuals.

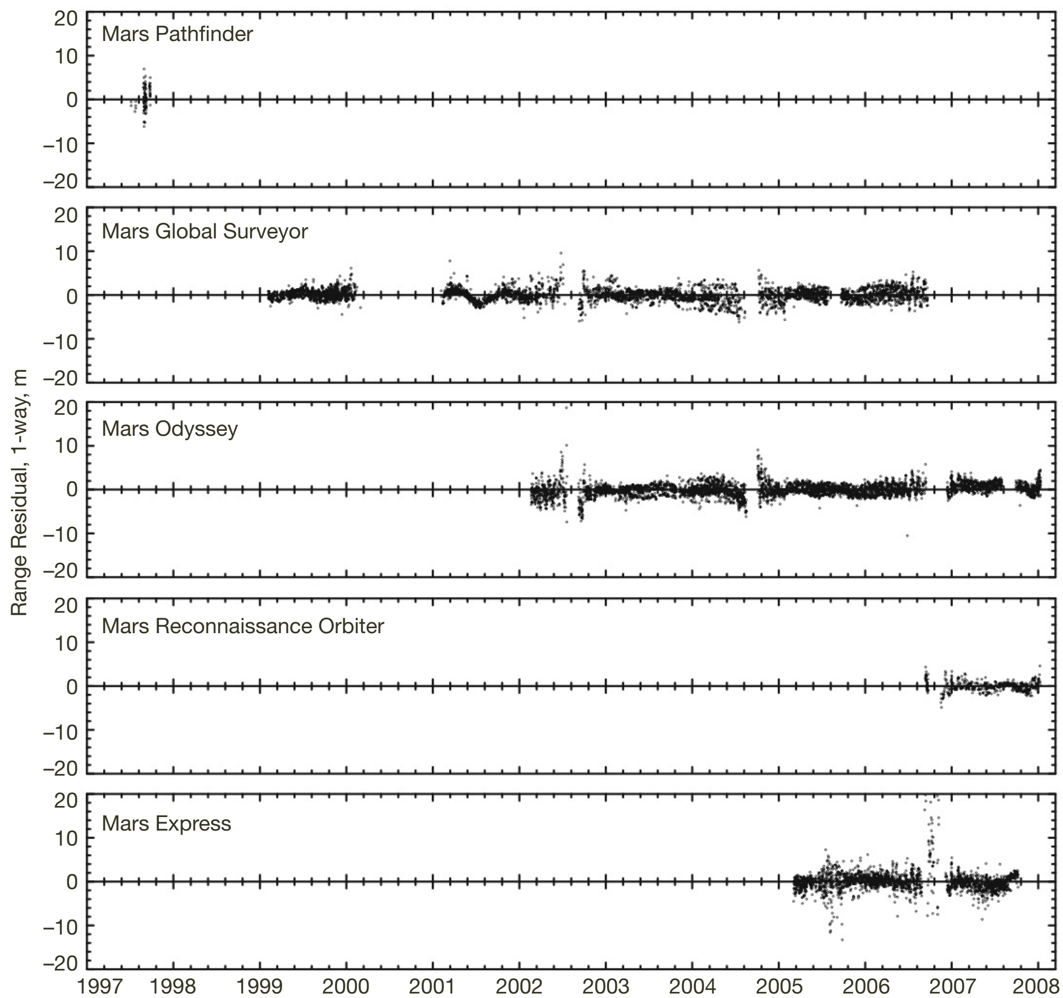

Figure B-11. Post-Viking Mars spacecraft range residuals.

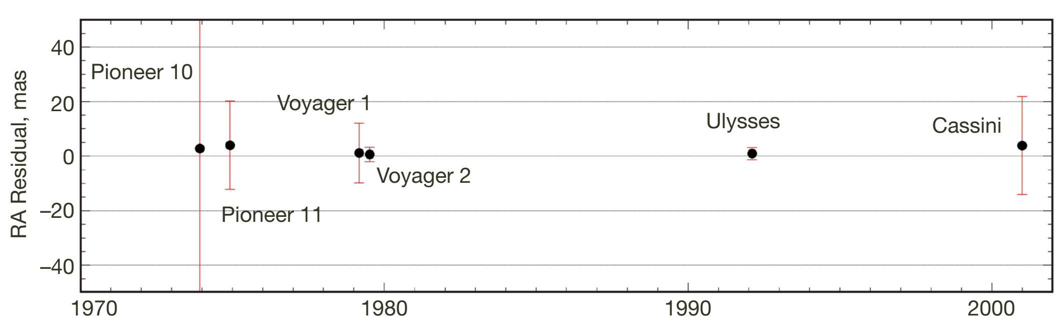

Figure B-12. Jupiter right ascension from spacecraft encounters.

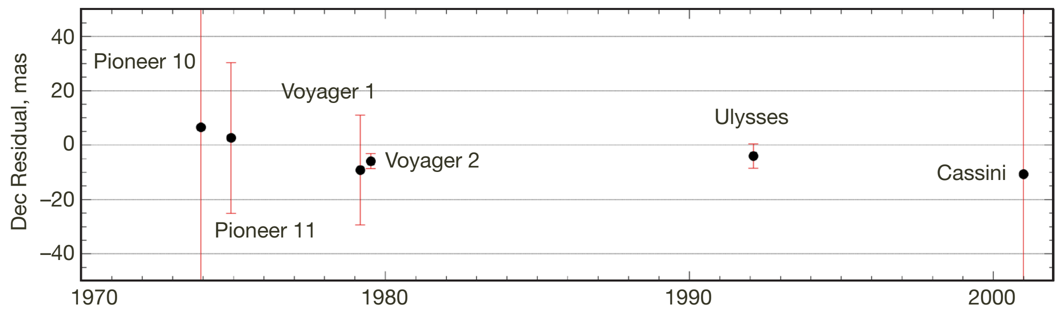

Figure B-13. Jupiter declination from spacecraft encounters.

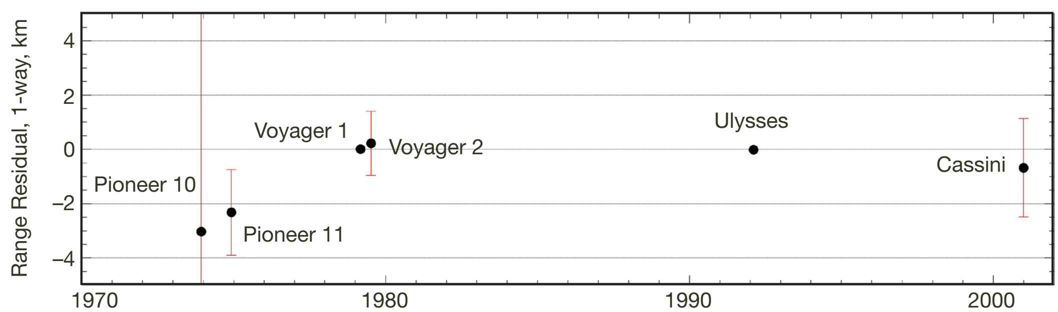

Figure B-14. Earth–Jupiter range from spacecraft encounters.

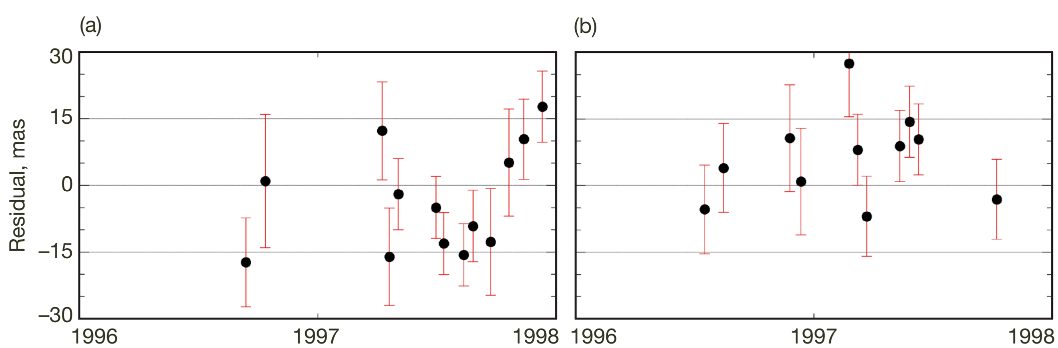

Figure B-15. VLBI observations of Galileo at Jupiter on (a) Goldstone–Canberra baseline and (b) Goldstone–Madrid baseline.

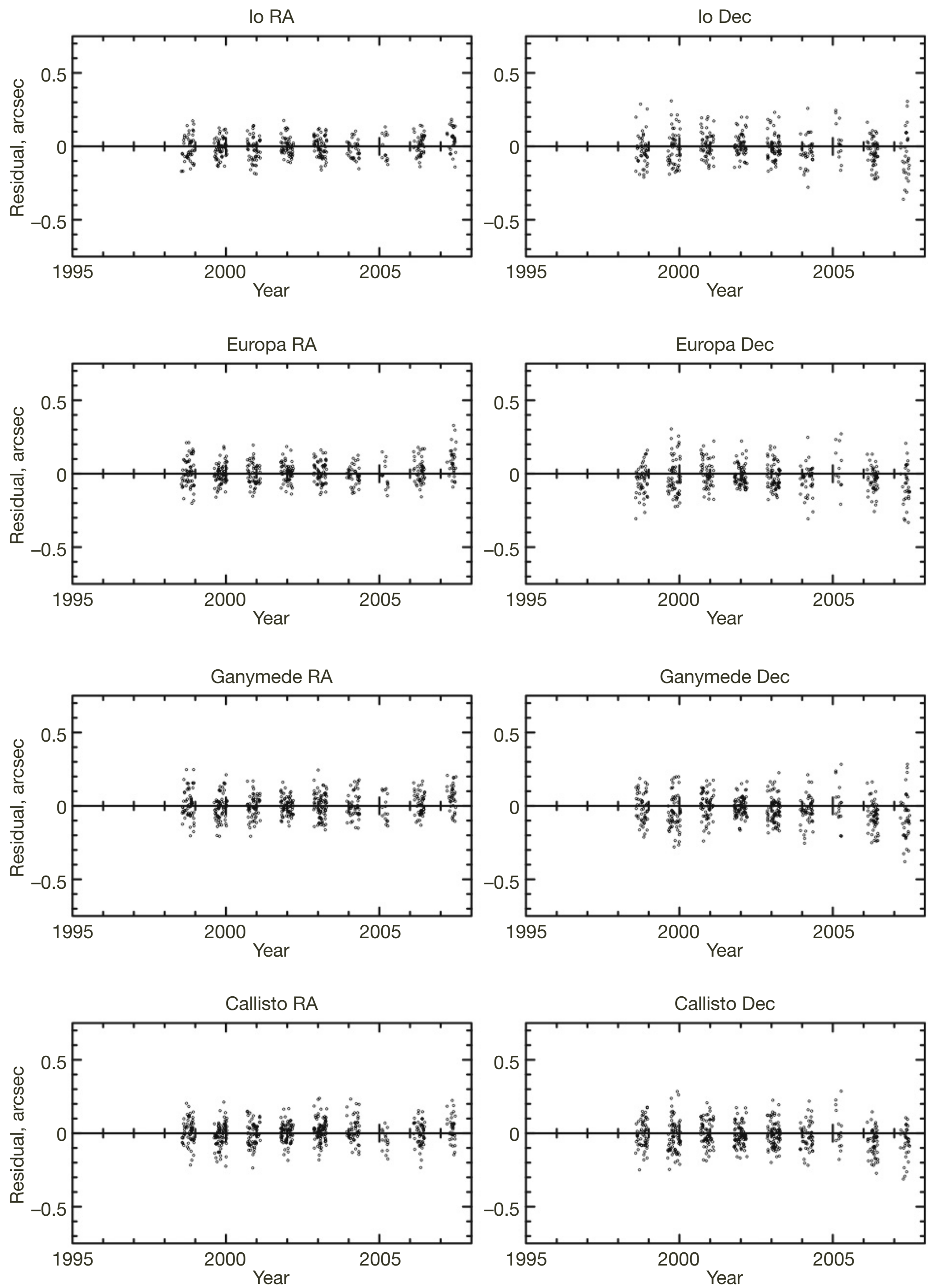

Figure B-16. Observations of Galilean satellites from U. S. Naval Observatory, Flagstaff.

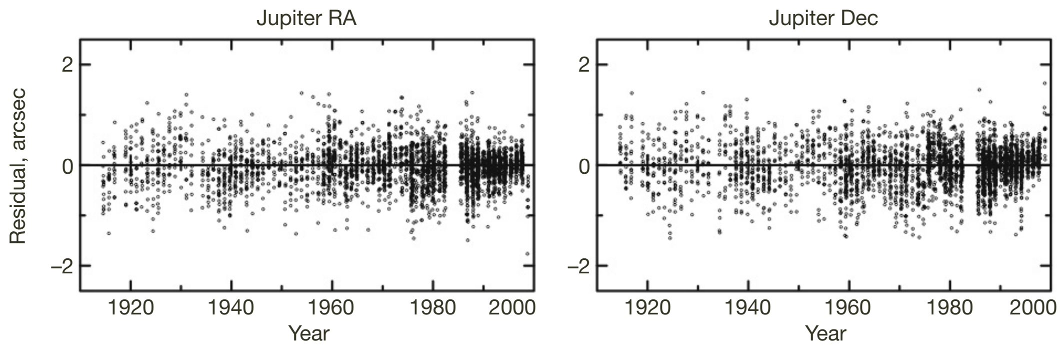

Figure B-17. Transit observations of Jupiter.

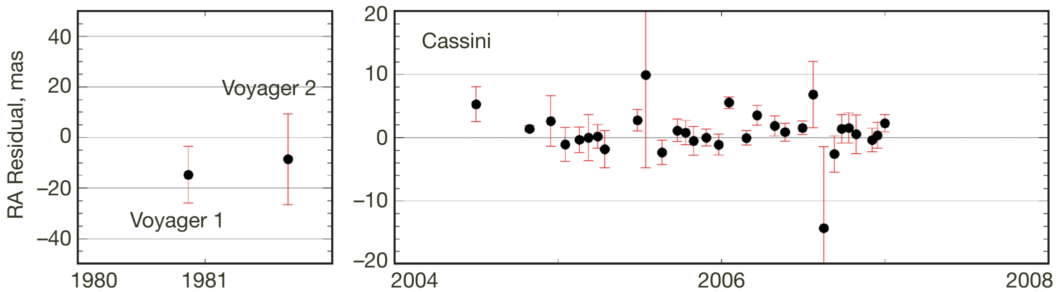

Figure B-18. Saturn right ascension from Voyager 1 and 2 and Cassini tracking analysis.

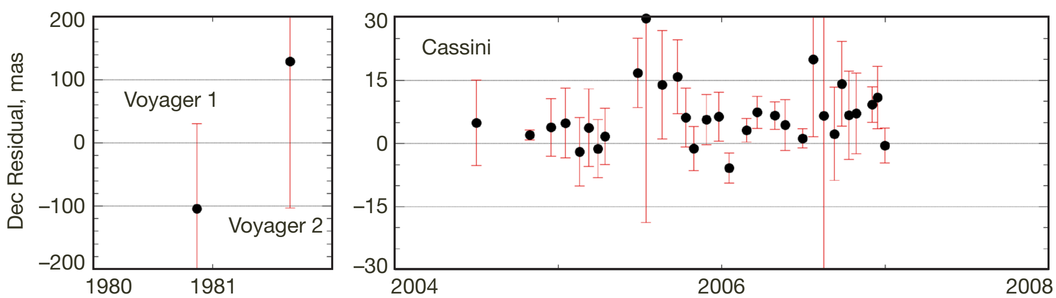

Figure B-19. Saturn declination from spacecraft encounters.

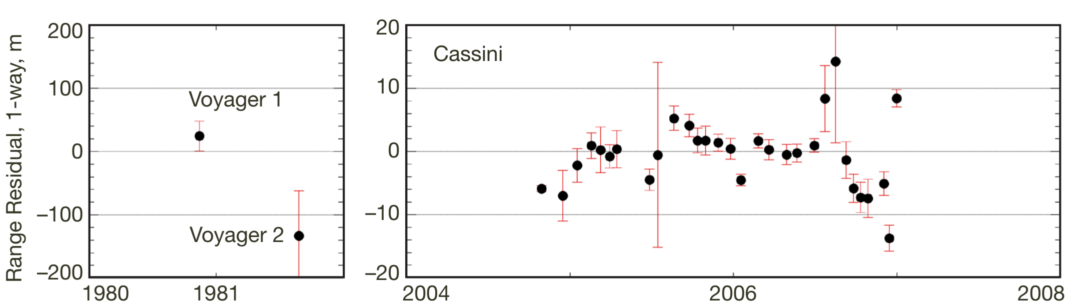

Figure B-20. Saturn–Earth range from spacecraft encounters.

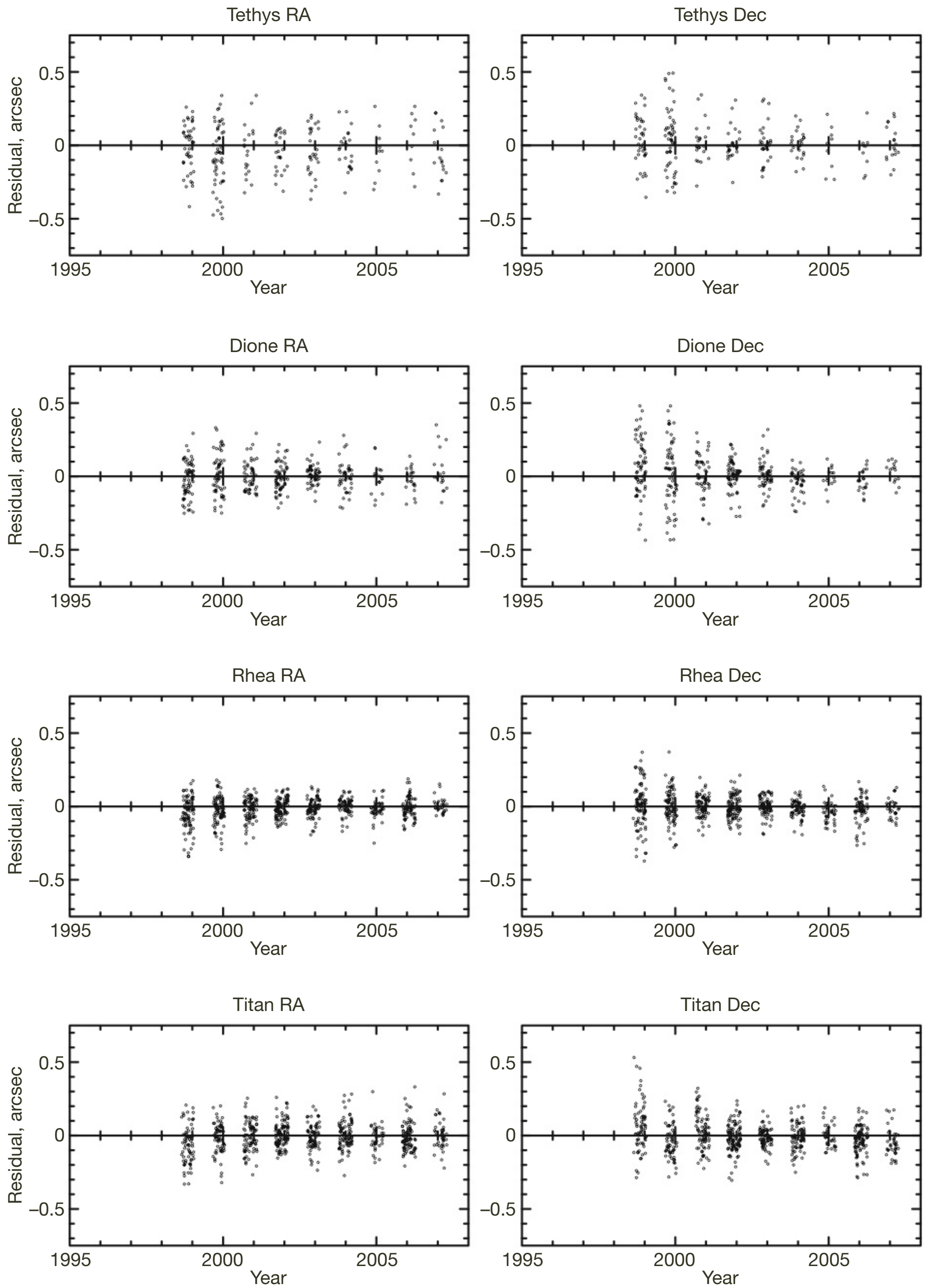

Figure B-21. Saturn satellite (3–6) observations from U. S. Naval Observatory, Flagstaff.

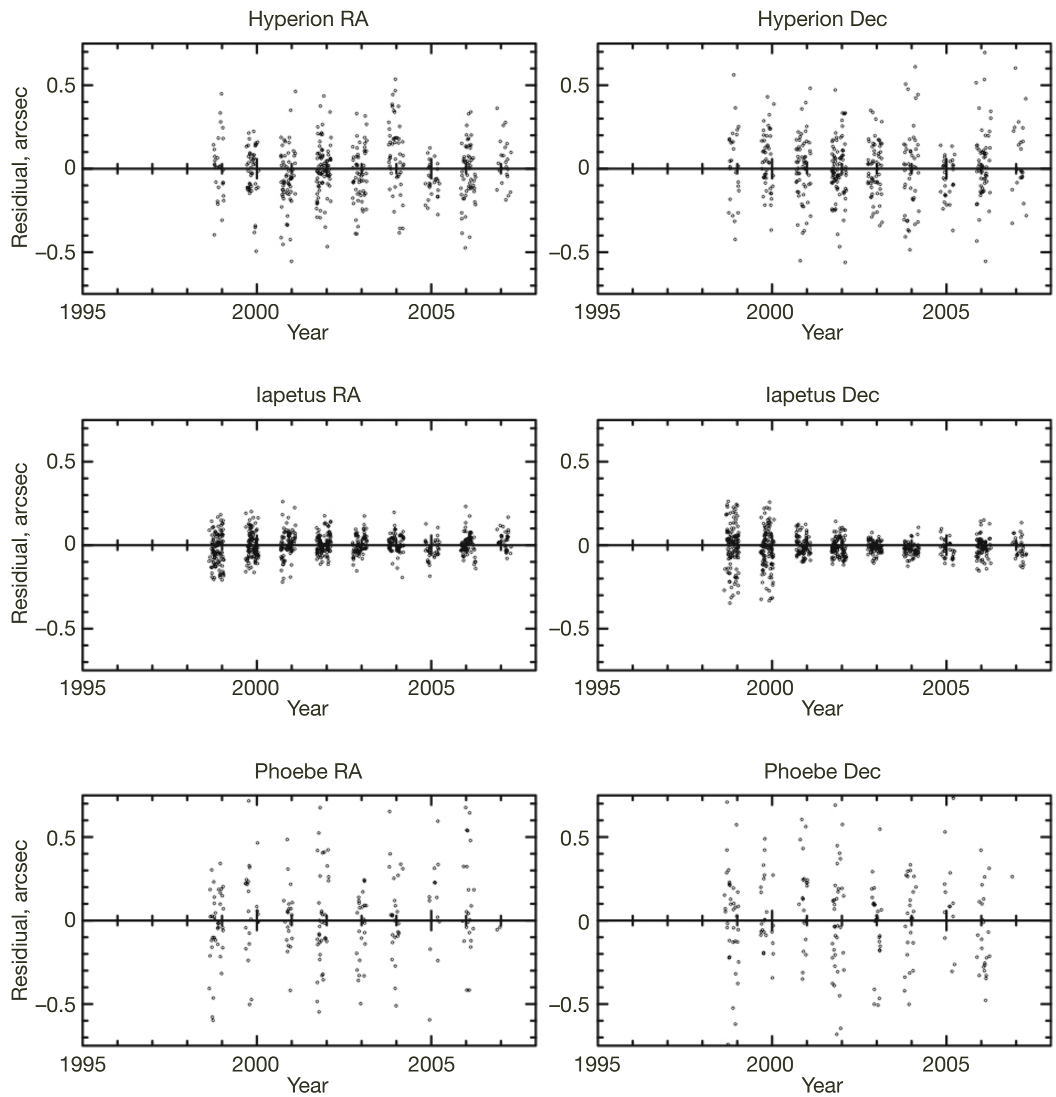

Figure B-22. Saturn satellite (7–9) observations from U. S. Naval Observatory, Flagstaff.

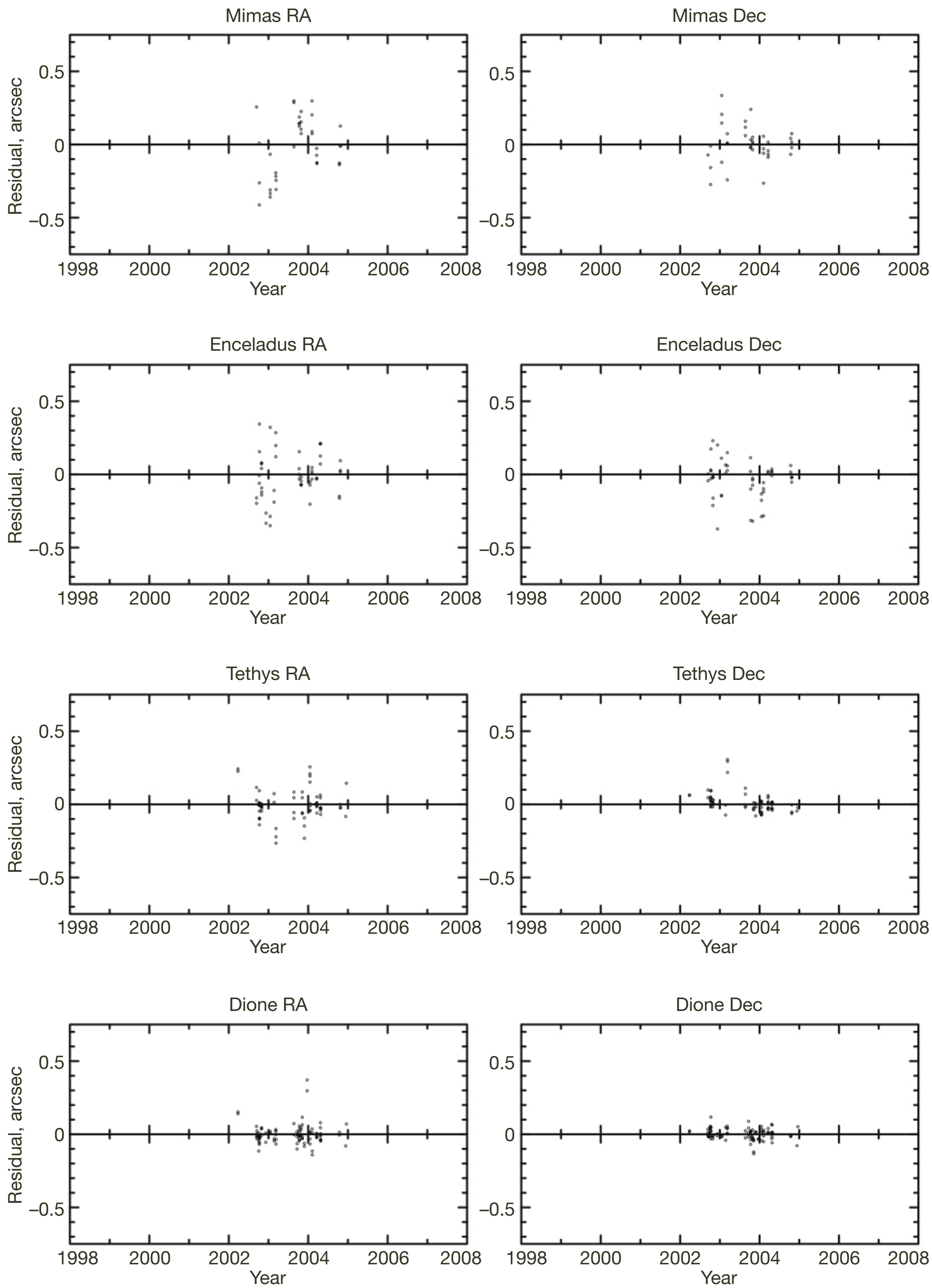

Figure B-23. Saturn satellite (1–4) observations from Table Mountain Observatory.

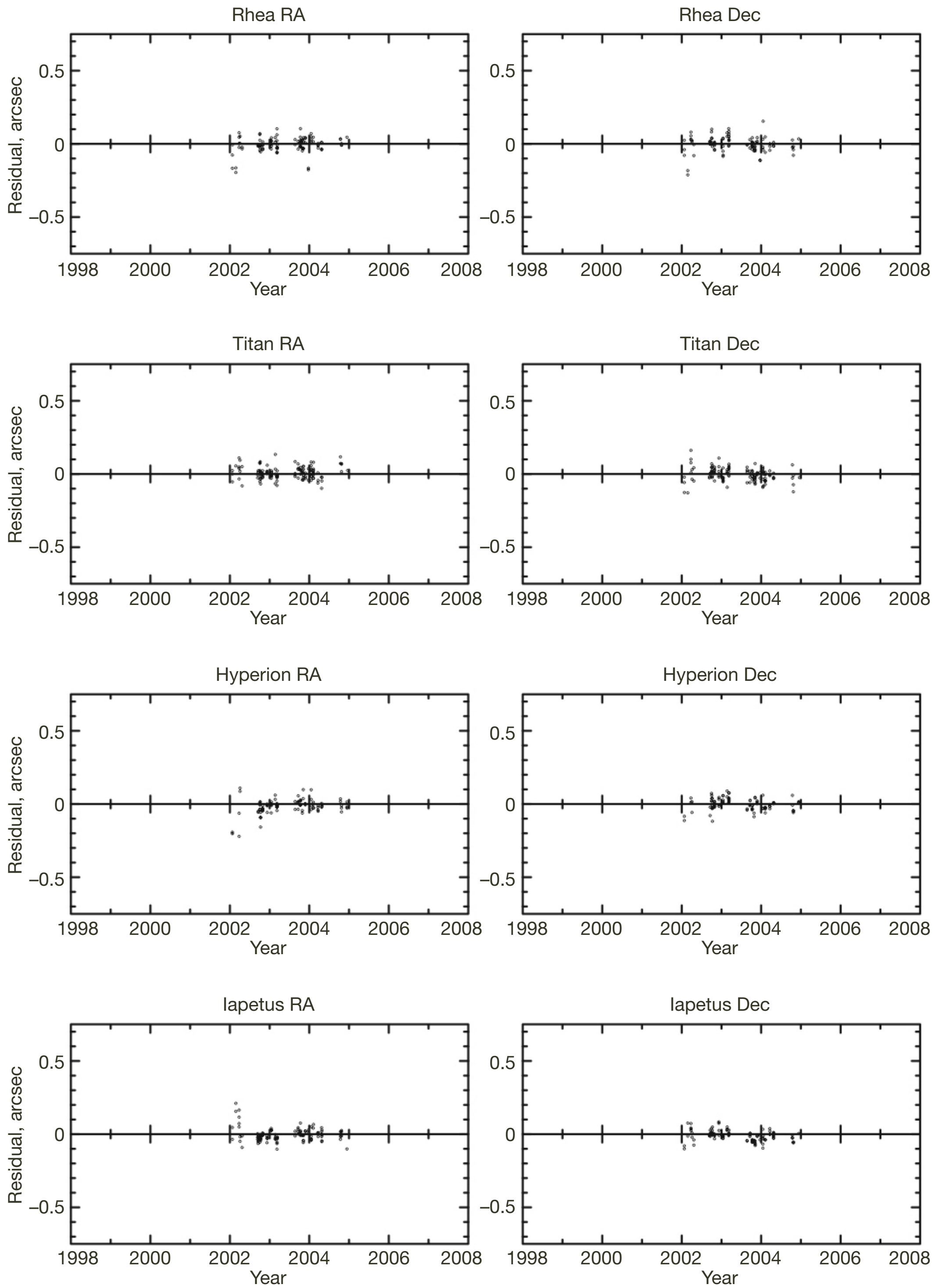

Figure B-24. Saturn satellite (5–8) observations from Table Mountain Observatory.

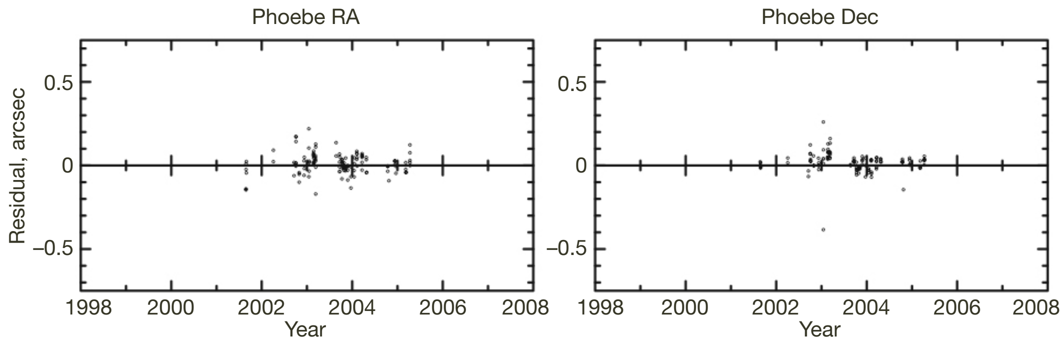

Figure B-25. Saturn satellite (9) observations from Table Mountain Observatory.

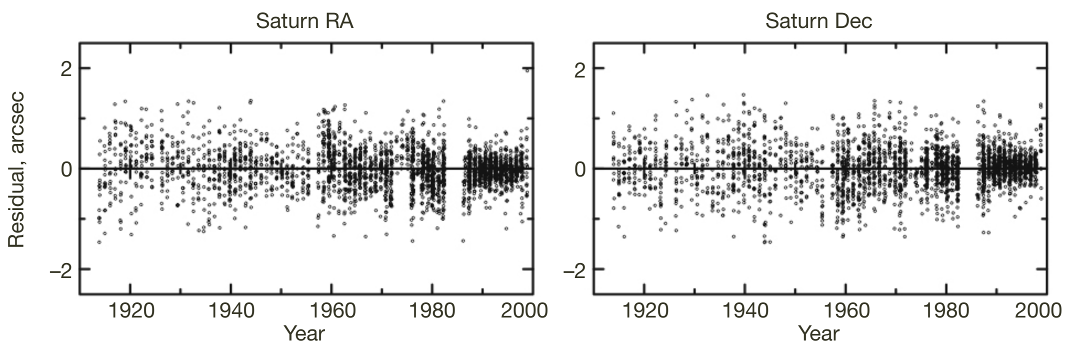

Figure B-26. Transit observations of Saturn.

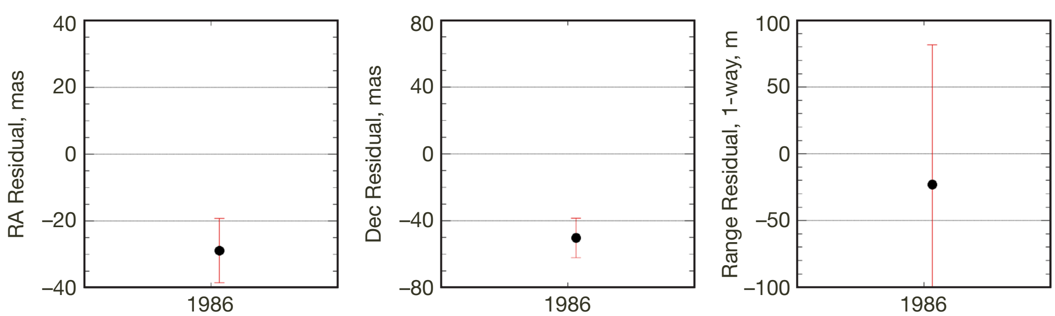

Figure B-27. Uranus right ascension, declination, and range from Voyager 2 encounter.

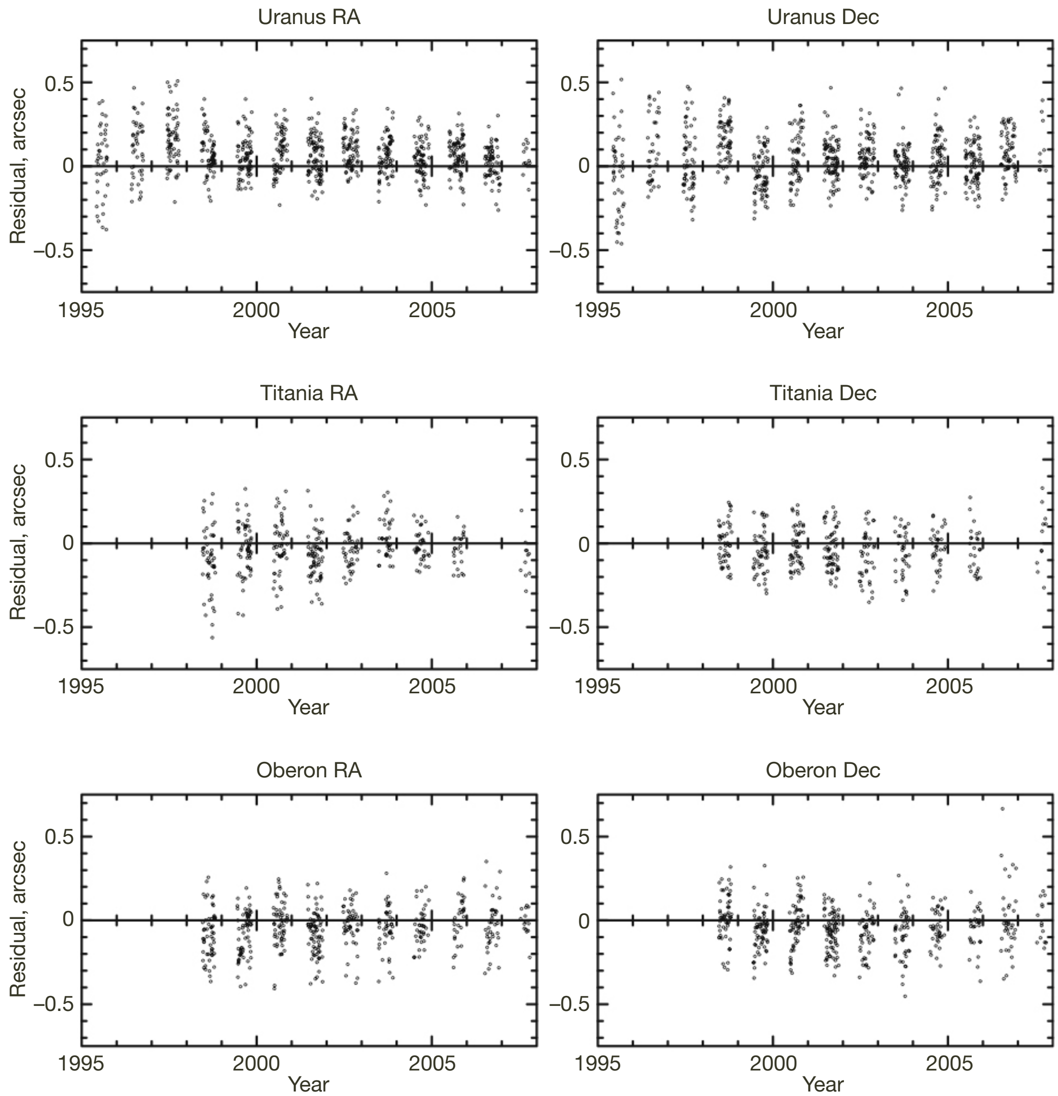

Figure B-28. Uranus observations from U. S. Naval Observatory, Flagstaff.

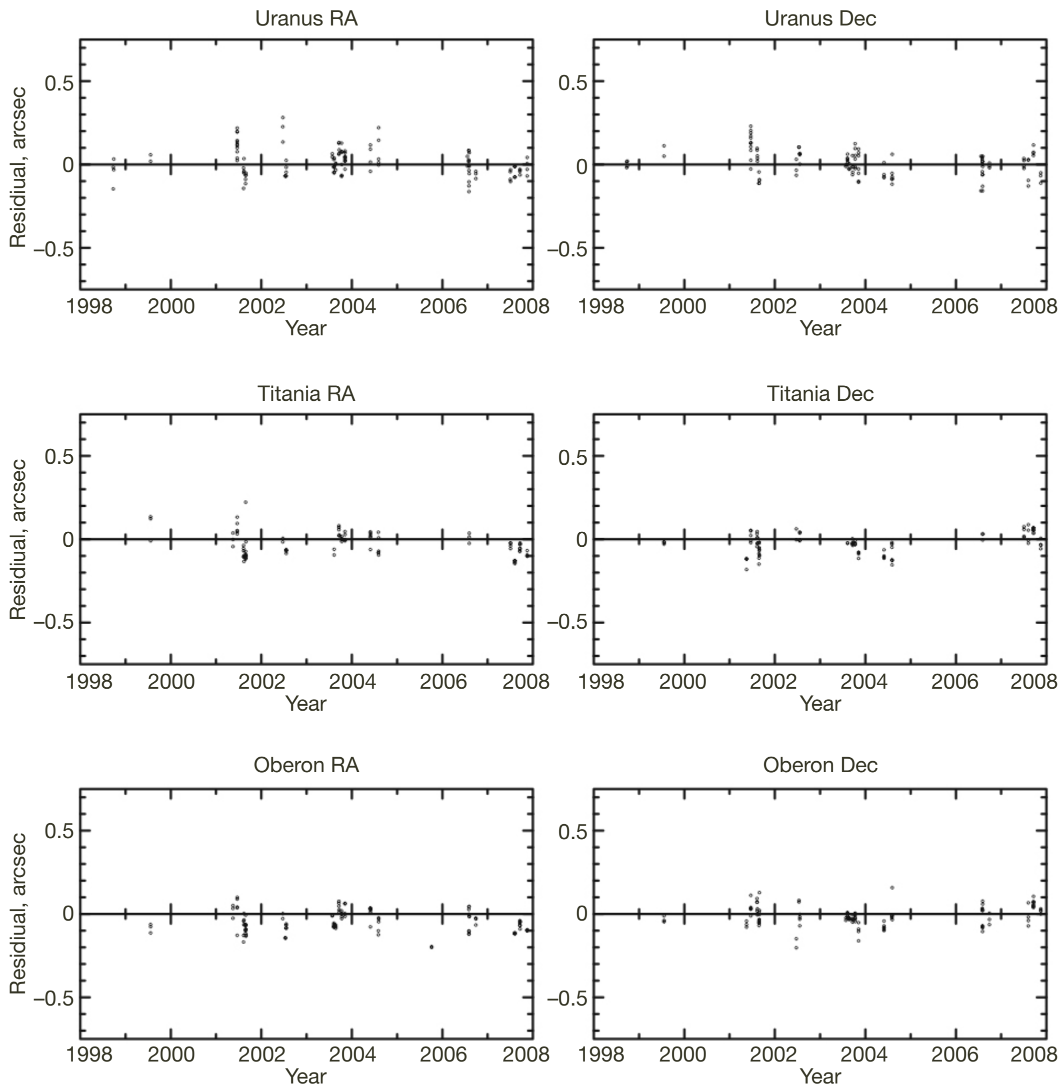

Figure B-29. Uranus observations from Table Mountain Observatory.

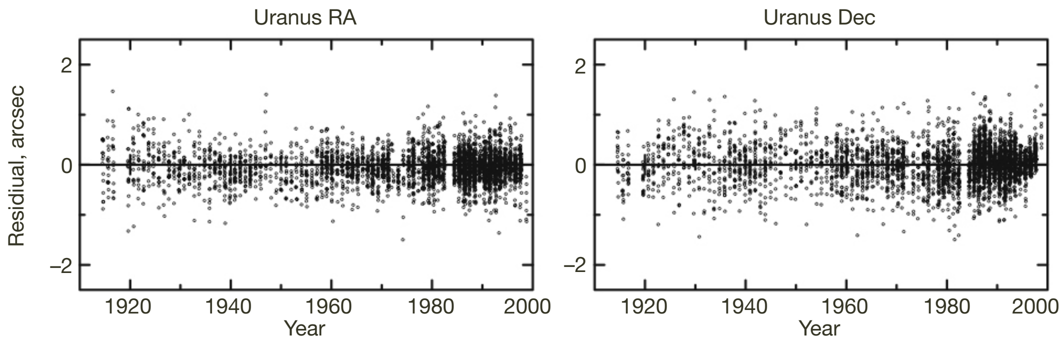

Figure B-30. Transit observations of Uranus.

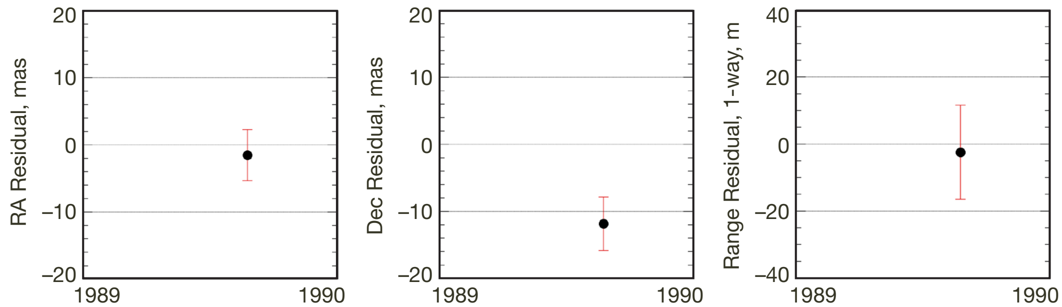

Figure B-31. Neptune right ascension, declination, and range from Voyager 2 encounter.

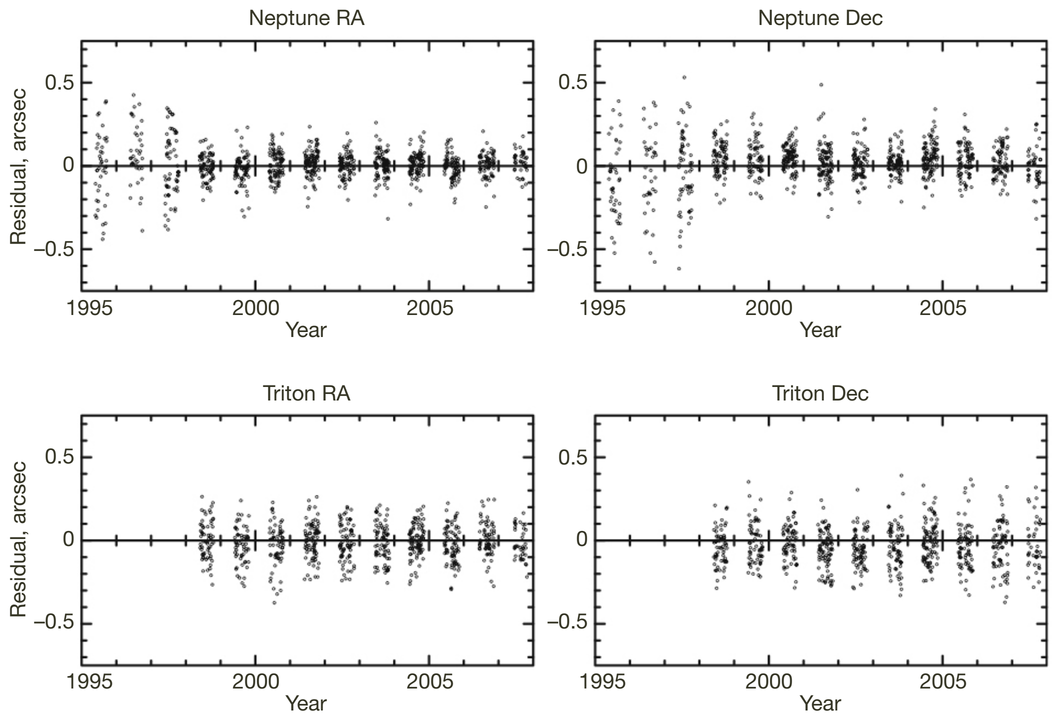

Figure B-32. Neptune observations from U. S. Naval Observatory, Flagstaff.

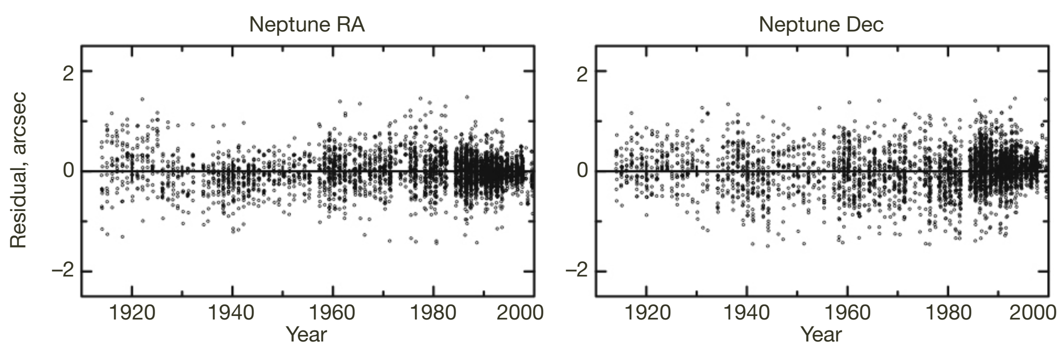

Figure B-33. Transit observations of Neptune.

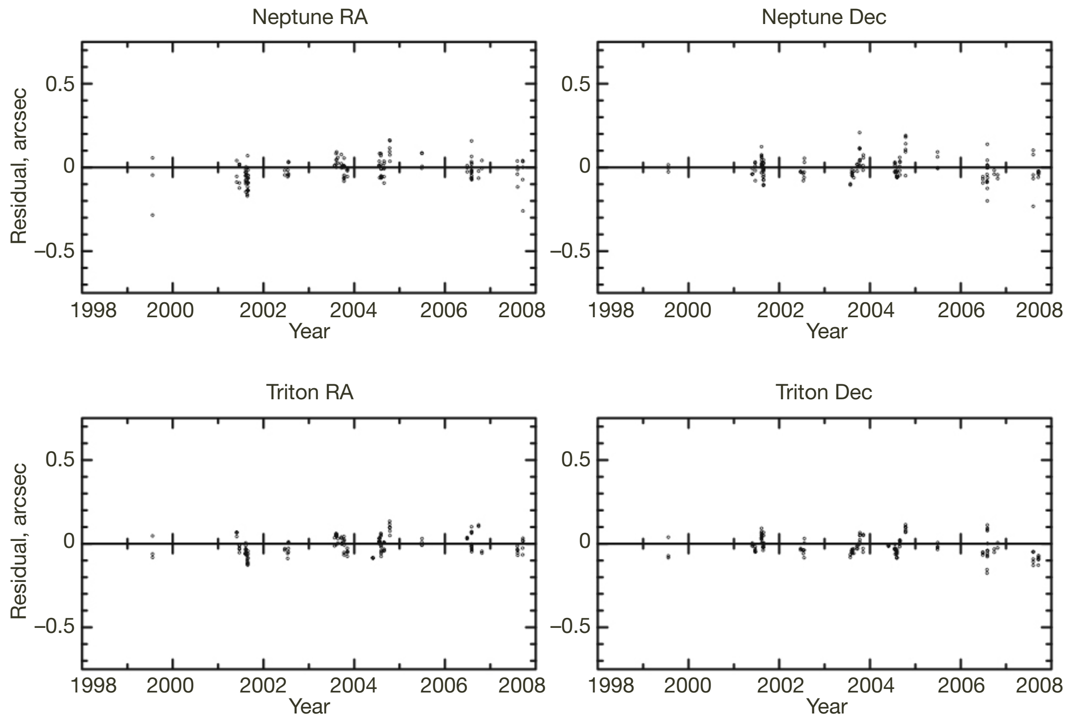

Figure B-34. Neptune observations from Table Mountain Observatory.

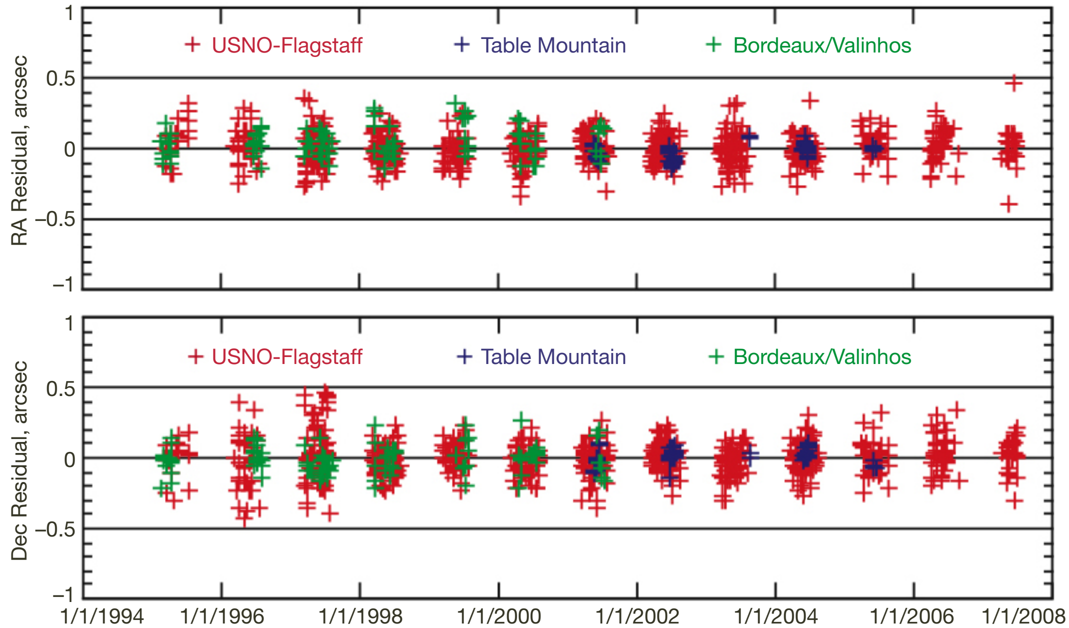

Figure B-35. Residuals of modern Pluto observations.

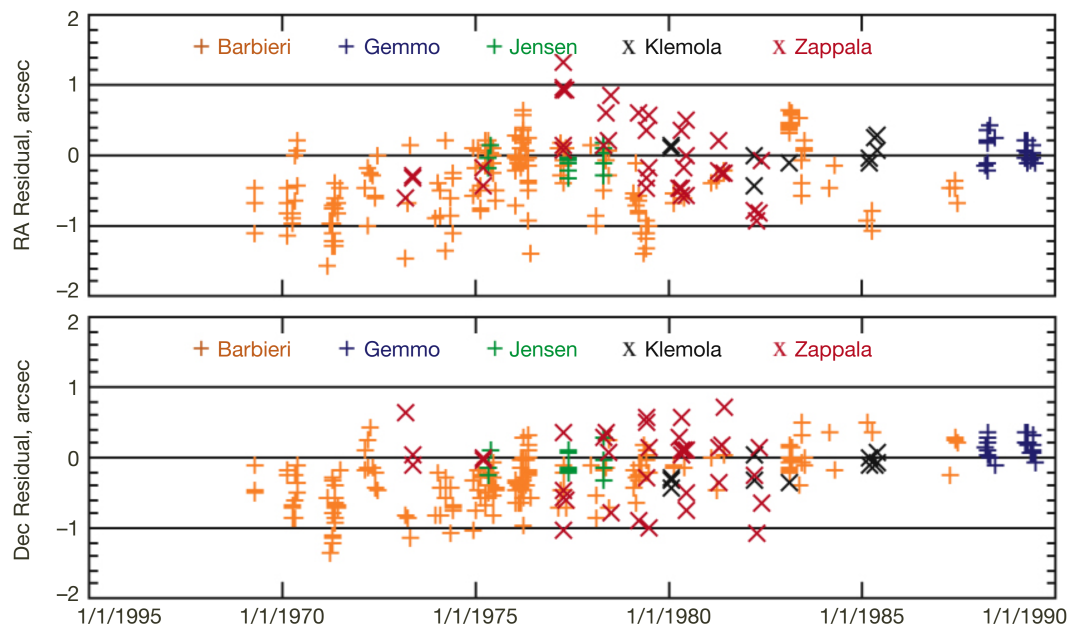

Figure B-36. Residuals of Pluto observations 1968–1990.

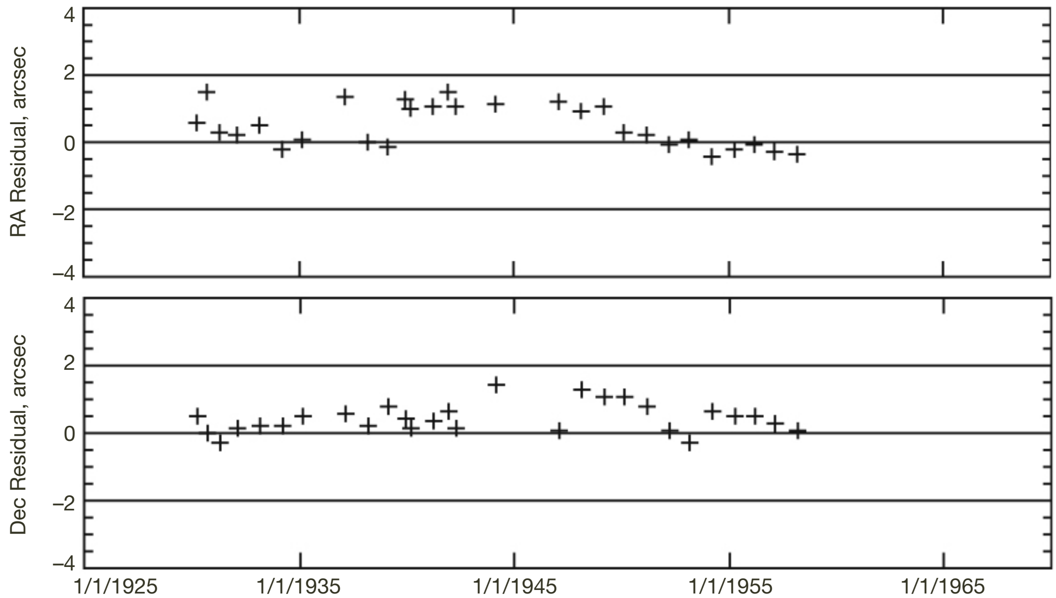

Figure B-37. Residuals of Pluto normalized points from Lowell, Yerkes, McDonald, etc.

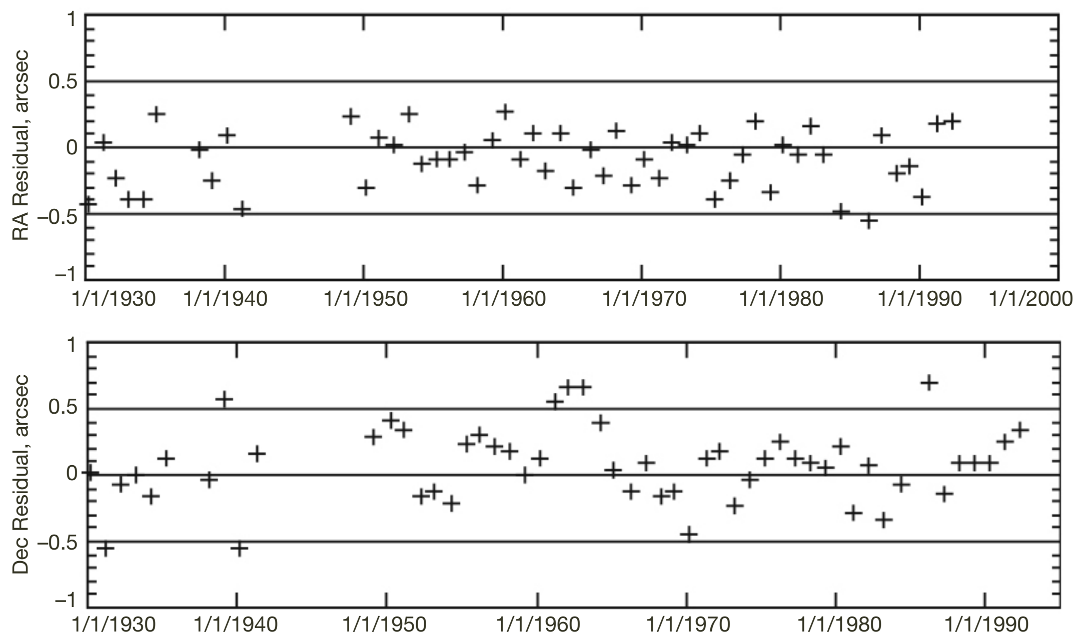

Figure B-38. Residuals of Pluto observations from Pulkovo astrograph.

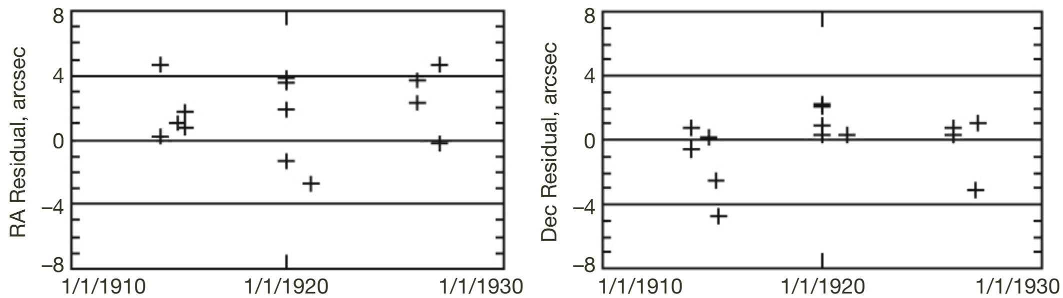

Figure B-39. Residuals of Pluto prediscovery observations.

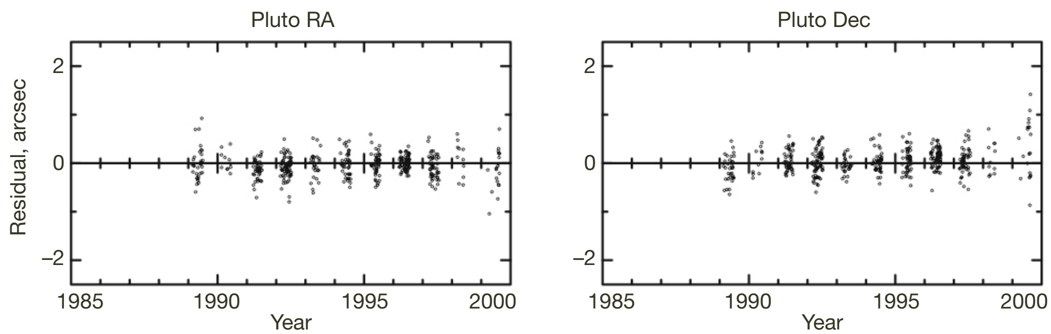

Figure B-40. Transit observations of Pluto.